КОНФЕРЕНЦИЯ
по
МОРЕХОДНЫМ КАЧЕСТВАМ СУДОВ
И ПЛАВУЧИХ ТЕХНИЧЕСКИХ СООРУЖЕНИЙ
Сентябрь 1983 Варна

CONFERENCE
on
SEAGOING QUALITIES OF SHIPS
AND MARINE STRUCTURES
September 1983 Varna



# EFFECTS OF SERVICE CONDITIONS ON PROPULSIVE PERFORMANCE OF SHIPS

H. Tanibayashi

## 1. INTRODUCTION

When we discuss the service performance of a ship, it should be borne in mind that it is certainly different from the trial performance which is usually pertaining to the condition of a clean hull in calm water without much wind. However, ships are ordinarily operating on a sea route which is not always calm, or more generally in wind and waves with her hull getting fouled after docking and further with unavoidable surface deterioration.

Shipowners have been well aware of this, and in defining service speed they have been taking these effects into account in terms of sea margin. The sea margin generally addresses the difference in propulsion power from that obtained at the time of speed trial (power margin). Further, it is generally known that the propeller rate of rotation is decreased when compared at the same power i.e. power identity (rpm margin). This also is called the sea margin which is to be taken into account for propeller design. These are schematically described in Figs.1.1 and 1.2.

Whilst the study on estimating and analyzing the propulsive performance of ships is progressed which has its basis on analytical consideration, it has become possible to describe such overall sea margin as defined in terms of power and rpm in a more analytical way. By 'analytical' it is meant in this paper that the overall power and rpm are calculated with individual effects of fouling, wind and waves assessed separately (Fig.3). This is an aspect of great advantage for analytical methods developed with wide applicability due to its flexibility in mind.

The paper is intended for describing a method for computing the sea margin for these individual factors. Amongst a number of analytical methods /1, 2, 3/, the ITTC 1978 Performance Prediction Method /4/ is chosen as a proto-type, and some extensions are attempted to adapt it to service conditions with a rational basis. In so doing, recent investigations on hull and propeller roughness, wind and wave effects, service performance prediction and analysis are reviewed and incorporated as well as those published in the past. Considering the readers' convenience for reference, figures illustrating the reviews are summarized on a single page for each item of description.

## 2. ITTC 1978 PERFORMANCE PREDICTION METHOD

Although the readers are presumed to be acquainted with the ITTC 1978 performance Prediction Method /4/, its essence is explained briefly in Table 1 to facilitate the understanding of the following chapters.

## 3. EFFECT OF ROUGHNESS DUE TO FOULING AND SURFACE DETERIORATION

Of the causes of roughness of the hull and propeller surface, fouling refers in this paper to a transient phenomenon which grows with time and can be removed at docking, while surface deterioration is a slow continuous process, called also ageing, which occurs progressively throughout the life of the ship and the propeller /5/.

The important parameters determining the effect of roughness are the height of the roughness in relation to the boundary layer thickness, and the density and the general shape of the roughness.

Up to the present, most investigations into the effect of roughness have been based on measurements of the roughness in terms of mean apparent amplitude for a 50 mm gauge length as defined by the BSRA method /6/. Measurements of the mean apparent amplitude have provided useful information, but recently several attempts have been made to incorporate a more precise definition of roughness.

In the following, these investigations into roughness effect are reviewed in regard to hull resistance, propeller characteristics and propulsion factors in connection with the recent strong demand for fuel economy.

### 3.1. Effect of Hull Roughness on Ship Resistance

The formula included in the ITTC 1978 method was derived from the full scale thrust measurements conducted by NPL and BSRA /7,8/. In the analyses the ship resistances were estimated using thrust values measured during ship trials making the assumption that the thrust deduction fractions for model and ship are the same. Although the accuracy of ship thrust measurements is sometimes questionable and the results showed a considerable scatter, reasonable trends could be established which indicated that:

1. The curves of $(C_F + \Delta C_F)$ values run parallel to, or approach the ITTC line as Reynolds number increases (Fig.3.1). The trends are different from Nikuradse's sand roughness curves (Fig.3.2, /10/) which attain a constant value with increasing Reynolds number.
2. For the same numerical values of uniform sand roughness k/L and hull roughness ($k_s/L$ ($k_s$: MAA), the resistance increment for hull roughness is much less than for Nikuradse's sand roughness converted to flat plate (Fig.3.3, /10/).
   [N.B.] According to the notation of ITTC 1978 Method, hull roughness is denoted by $k_s$ to make difference from propeller roughnes $k_p$. Therefore Nikuradse's sand roughness (usually expressed by $k_s$) is denoted by k in this paper except for Figs.3.2 and 3.3 cited from reference /10/.
3. The variation of ship resistance increment may be estimated from

$$10^3 \Delta C_F = 105(k_s/L)^{1/3} - 0.64 \qquad (3.1)$$

as shown in Fig.3.4.

The suitability of this equation was shown by the analysis of correlation data made by the 14th ITTC Performance Committee. This equation with $k_s$ taken $150 \times 10^{-6}$ m constant made an important contribution in reducing the scatter of the data from many of the tanks /11/. It should be noted in this context that the formula (3.1) included in the ITTC 1978 method is a function of L alone, and does not depend on $k_s$.

How about then to regard this equation as a functuion of the roughness $k_s$? In recent years a number of laboratory investigations have been carried out to determine the resistance of replicas of typical hull surfaces or those similar to them, using a floating element balance /12/, transfer to the interior of pipe flow /13, 14/, towing a flat plate in a towing tank /15/ or mounting it in a flume /16/.

According to Clauser /17/, effect of roughness can be expressed by downward velocity shift $\Delta u/u_o$ in the velocity distribution in the boundary layer as shown in Fig.3.5, where u is the local mean velocity and $u_o$ is the shear velocity defined by $\sqrt{\tau/\rho}$. Once this $\Delta u/u_o$ is known as a function of roughness profile and Reynolds number of the flow, as called roughness function illustrated in Fig.3.6, the local skin friction can be claculated by

$$\left(\sqrt{\frac{2}{C_F}}\right)_{rough} = \left(\sqrt{\frac{2}{C_F}}\right)_{smooth} - \frac{\Delta u}{u_0} \qquad (3.2)$$

Model drag data of a roughened plate can be extrapolated by Sasajima-Himeno's formula

$$\Delta C_{FS} = \Delta C_{FM} \left(\frac{C_{FS}}{C_{FM}}\right)^2 \qquad (3.3)$$

with roughness Reynolds number $Uk/\nu$ = constant /18/.

Fig.3.7 shows the results from the above method of calculation and the extrapolation of the model data applied to a full ship form of 220m in length /15/. Both results are found to be in good agreement with one another, and they can be approximated by the line 1/4 or 1/5 of Nikuradse's sand roughness.

Evidently, however, these data are much different from the ITTC 1978 correlation formula. Plotting the data points comprising this formula, it can be seen that they are confined to the range of roughness not larger than 280 × $10^{-6}$ m and therefore may not be extrapolated to such a range of roughness as found in Fig.3.8 for general service conditions. Another point to be noted with this plotting is that the NPL-BSRA data give generally large $\Delta C_F$ even in the small roughness range. This may be due to that the NPL-BSRA data include the effect of structural roughness, difference between actual and formulated ship's resistance coefficients etc., whereas $\Delta C_F$'s obtained by calculation or model experiments are concerned with incremental resistance due to hull surface roughness.

Recently an empirical formula was proposed for assessing power increase resulting from roughness increase such as /19/,

$$\Delta P/P = 3.8\left[(k_{sz})^{1/3} - (K_s)^{1/3}\right] \quad (3.4)$$

(%) $K_s$ in microns

A sample calculation for the ship shown in Fig.3.7 indicated that the power increase estimated by this formula (3.4) corresponds approximately to Nikuradsé-Schlichting's k = 1/4 $k_s$ line.

Theory of the flow over a rough surface is a topic attracting many investigations, reflecting recent economic demand for fuel saving. The recent work by Grigson /20/ indicates that the roughness function can be determined, regardless of the details of the surface topography, simply by

$$A \log (1 + \overline{h}_+/m) \quad (3.5)$$

where $\overline{h}_+$ is a mean value of peak-to-trough roughness height and m is a parameter representing wave length found by experiment (Fig.3.9).

Another important factor to be studied in connection with surface roughness is the effect of fouling. This is primarily due to slime and barnacles which grow with time after docking, and their effect on propulsive performance has been known to be significant. The problem is, however, that it is difficult to define the surface characteristics to the extent of quantitative presentation. The slime is a highly viscous liquid attached to the hull after soaking in a dead water, and it is measureable only within a short period of time after the surface has been lifted out of water. Therefore only a few model data are available at present as illustrated in Figs.3.10 and 3.11 /21/ Barnacles as shown in Fig.3.12 are so diverse with its kind, the circumstances under which it grows, and the operation patterns of a ship, and so it is difficult to define the loss in the propulsive performance for a specific type and extent.

## 3.2. Effect of Roughness of Blade Surface of a Propeller

In the ITTC 1978 method, the roughness of the blade surface of a propeller is assumed to be a constant value of 30 × $10^{-6}$ m. If this assumption is relieved to adapt for an arbitrary value of roughness kp, its effect is calculated according to the formulae /23/,

$$C_{DM} = 2\left(1+2\frac{t}{c}\right)\left[\frac{0.044}{(R_{nco})^{1/6}} - \frac{5}{(R_{nco})^{2/3}}\right] \quad (3.6)$$

$$C_{DS} = 2\left(1+2\frac{t}{c}\right)\left(1.89+1.62\cdot\log\frac{c}{k_P}\right)^{-2.5} \quad (3.7)$$

The difference in drag coefficient $\Delta C_D$ is

$$\Delta C_D = C_{DM} - C_{DS} \quad (3.8)$$

and

$$\Delta K_T = -\Delta C_D \cdot 0.3 \cdot \frac{P}{D} \cdot \frac{c \cdot z}{D} \quad (3.9)$$

$$\Delta K_Q = \Delta C_D \cdot 0.25 \cdot \frac{c \cdot z}{D} \quad (3.10)$$

The roughness term in the eq. (3.7) above was taken from the frictional coefficient of a flat rough plate as calculated by Prandtl and Schlichting /10/ on the basis of Nikuradse's pipe experiments (Figs.3.2 and 3.3). Within the range of Reynolds number and roughness concerned, this is independent of Reynolds number and is expressed as a function of relative roughness alone.

Fig.3.13 shows a sample calculation according to the formulae (3.7) - (3.10) on a propeller of a tanker, in which the roughness was varied up to 1000 × $10^{-6}$m. This was done by Meyne /23/. As indicated by this figure, effect of roughness on $K_T$ is relatively smaller than on $K_Q$. In order to look at a genenral tendency of propeller efficiency as a function of the surface roughness of the blades, approximate calculation was made based on the above equations (3.7) - (3.10).

By the definition of open-water efficiency

$$\frac{\Delta\eta_0}{\eta_0} = \frac{\Delta K_T}{K_T} - \frac{\Delta K_Q}{K_Q} \qquad (3.11)$$

and replacing $\Delta K_T$ and $K_Q$ by $C_D$, we get

$$\frac{\Delta\eta_0}{\eta_0} = -\left(\frac{0.3}{K_T}\cdot\frac{P}{D} + \frac{0.25}{K_Q}\right)\cdot\frac{C}{D}\cdot Z\cdot\Delta C_D \qquad (3.12)$$

Numerical calculation was performed on the following conditons

$D = 7.0^m$, $C/D = 0.3$ $Z = 5$

for a tanker

$K_T = 0.2$, $K_Q = 0.02$, $P/D = 0.7$

for a container ship

$K_T = 0.2$ $K_Q = 0.04$, $P/D = 1.2$

The results are shown in Fig.3.14, where the base of efficiency $\Delta\eta_0 = 0$ was taken at $kp = 30 \times 10^{-6}m$.

For practical application of these results to service performance of ships, it is desirable to compare them with experimental results.

Meyne /23/ compared the calculated efficiency with some of those published on measurement data (Fig.3.15). Looking at the difference, he attempted to find an equivalent Nikuradse sand roughness as shown in Fig.3.7. The results indicate that, in contrast to the case of ship's hull, the apparent roughness of the measured data exhibits larger effect than the sand roughness of equal figures.

There are some other publications showing the effect of surface roughness on propeller characteristics, but only few data are available quantifying the surface roughness of the tested propellers, as shown in (Figs. 3.16 - 18, /24 - 27/).

To the author's knowledge, most extensive investigation made up to the present on this problem will be the one made by BSRA based on the measurement on over 130 propellers during the last 30 years. An approach similar to that for hull roughness has been extended to propeller roughness, but with numerical values transformed to the bandwidth and texture parameter appropriate for propeller blade surface. Of the measurement results, Rtm (2.5)---mean peak to valley height for a cut-off length of 2.5 mm---is plotted against age of propeller in Fig.3.19 /27/.

A texture parameter $\alpha$ is defined, as a measure of wave number, by the first three even moments of the spectrum of a profile

$$\alpha = \frac{m_0 m_2}{m_2^2} \qquad (3.13a)$$

or $$\alpha = \left(\frac{D_E}{D_Z}\right)^2 \qquad (3.13b)$$

where $D_E$ is the density of extrema and $D_Z$ is that of zero-crossing.

The mean values of this texture parameter increase, as shown in Fig.3.19. With repolishing, $\alpha$ increases in general, viz., deteriorating texture, while roughness decreases.

With thus defined roughness height and texture parameter, the roughness function can be obtained which describes the velocity defect in the boundary layer due to the roughness. According to Byrne et al /27/, this is expressed by

$$\frac{u}{u_0} = \frac{1}{K}\,\ell n\left(1+\frac{Rtm(2.5)u_0/\nu}{t}\right) \qquad (3.14)$$

where K = Kármán constant
$u_0$ = frictional velocity
t = texture parameter relating to Nikuradse's k

Fig.3.20 presents $K_T$, $K_Q$ curves for a smooth propeller and for several values of $R_{tm}$ (2.5) /t ranging from 1 to 100. Fig 3.21 shows the percentage increase in power for range of $R_{tm}$ (2.5)/t values for a container ship. From this figure it may be seen that at a service speed the power loss would be within 3 % to 4 % for most of the propellers observed.

Large penalty due to roughness of a full scale propeller was reported by Hundley /29/. This is a purely empirical data obtained from service performance of navy ships subject to scheduled cleaning. According to this report, efficiency loss of the propeller amounts to as high as 8 % (Fig.3.22). This value is considerably larger compared with the calculation such as shown in Fig.3.21. To correlate both, more other factors such as fouling with barnacles have to be taken into consideration.

Though somewhat apart from roughness, deformation of propeller blades due to cavitation erosion also has an appreciable effect on propeller characteristics. This is more so since most of the cavitation damage occurs near the trailing edge of the blades resulting in the bending. As indicated in Fig.3.23 /30/, a slight

bending causes a change of effective pitch which tends to decrease the rate of rotation of the propeller at constant power, though the power increase at the constant speed is neglible.

### 3.3. Effect of Hull Roughness on Propulsion Factors

In view of the resistance increase with hull roughness, it is intuitively inferred that the wake fraction will also increase with hull roughness corresponding to the momentum loss due to the hull resistance.

Model propulsion tests on artificially roughened hull have been carried out by R.E. Froude and Gawn on a liner model roughened with calico /36/, by Harvald et al on a bulk carrier model roughened by a sand strip /31/, and by Tokunaga on a VLCC model with nylon mesh /32/.

The first two papers report increase of model wake fraction with roughness as shown in Fig.3.24 - 25. Tokunaga conducted resistance test as well as the propulsion test, and showed that thrust deduction and relative rotative efficiency do not change with hull roughness (Fig.3.26). He showed further that the roughness in the after quarter is dominant for the increase of wake fraction. This is in agreement with the results of velocity measurements in the plane of propeller (Fig.3.27).

No data are available for wake fraction of roughened full-scale ships. There would be a possibility to estimate this from the full-scale measurement such as /8/ as a counterpart for $C_F$ analysis, but this will be subject to difficulty arising from that $\Delta W = W_M - W_S$ may not be a simple function of roughness but also of hull form.

## 4. EFFECT OF WIND AND SEAS

### 4.1. Effect of Wind on Hull Resistance

Performance of ships is affected by wind in terms of

(a) Wind resistance of the ship's above-water parts, and

(b) Wind induced resistance on the ship's under water hull. This is caused by a rudder angle and a drift angle to compensate the yawing moment due to the wind effect on the above-water parts.

It should be remembered further that the added resistance increases propeller loading and thus influences the propeller efficiency, but these effects can be taken into account by the ITTC 1978 method as explained later.

Wind coefficients for the ship's above-water parts, i.e, axial force, transverse force and yawing moment coefficients are in general obtained from wind tunnel tests with scaled models such as shown in Figs.4.1 and 4.2. Since wind tunnel testing is not usually carried out for every ship, data for ships with similar above-water configuration or some calculation method, such as Isherwood's /34/, may be used. Several investigations of wind coefficients have been published and provide useful information for a variety of ships, (cf. Wagner /35/, van Berelkom /36/, Tsuji /37/ etc.)

Of the wind coefficients of an above-water part, the axial component is of primary concern for propulsive performance of the ship. This is denoted usually by

$$C_X = \frac{X}{\frac{1}{2}\rho_a V_R^2 A_T} \qquad (4.1)$$

and plotted to the base of angle of incidence as shown in Figs.4.2 /34/. These coefficients are varied with type of ships, but it would be noted that the pattern of variation with the angle of incidence is more or less similar to each other. If this tendency is taken out by the wind direction coefficient,

$$k(\theta) = \frac{C_X(\theta)}{C_X(0)} \qquad (4.2)$$

then the $C_x$ at an arbitrary direction can be estimated if only the ahead resistance coefficient $C_x(0)$ is known. The curve of $k(\theta)$ which has been in use long since proposed by JTTC /38/ is shown in Fig.4.4. This is a curve obtained as an average of model test results on cargo ships and tankers up to 1940's, but it would be interesting to note that inclusion of modern data collected by Wilson and Roddy /39/ still yields much the same tendency as shown in Fig.4.5.

According to Wagner /35/ and others, typical values of the ahead resistance coefficient may be taken as follows.

| | |
|---|---|
| Tanker | 0.8-1.0 |
| Cargo ship | 0.6-0.8 generally smaller in light condition than loaded |
| Coasters | 0.85-1.0 |
| Passenger boat | 0.3-0.4 |

Isherwood /34/ analyzed the wind resistance experiments carried out at several different test establishments on models covering a wide range of merchant ships. As a result, he gave equations for estimating the components of wind force and moments on any merchant ship form for a wind from any direction as functions of geometrical particulars of a ship. For example, wind resistance coefficient is expressed by

$$C_X = A_0 + A_1 \frac{2A_L}{L_{OA}^2} + A_2 \frac{2A_T}{B^2} + A_3 \frac{L_{OA}}{B} \quad (4.3)$$

where $L_{OA}$ = length overall
$B$ = beam
$A_L$ = lateral projected area
$A_T$ = transverse projected area

For the ahead wind $\theta = 0$, the coefficients A's are as follows.

$A_0 = 2.152$
$A_1 = -5.00$
$A_2 = 0.243$
$A_3 = -0.164$

In the ITTC 1978 method, the effect of air resistance is taken into account by

$$C_{AA} = 0.001 A_T/S \quad (4.4a)$$

Considering $\rho air/\rho water = 1/836$, this corresponds to

$C_x = 0.85$
$V_R = V_s$

Wind speed equals ship speed, viz. ship advancing in no wind. For arbitrary wind force and direction, this is replaced by

$$C_{AA} = \frac{C_X}{836} \frac{V_R^2}{V_S^2} \frac{A_T}{S} \quad (4.4b)$$

When the relative wind is not on the bow ($\theta = 0^\circ$) or stern ($\theta = 180^\circ$), the ship will experience a lateral force and a yawing moment. This force and moment must be balanced by the hydrodynamic forces and moments on the ship's under-water hull. It is first assumed that the wind is steady and consequently the wind forces are constant, so that the counteracting hydrodynamic force and moment may be obtained from a constant drift angle (or constant sideslip) and a constant rudder angle.

These are generally obtained by oblique tow test and rudder angle test, respectively, but there are not many published data available. According to Norrbin /40/, the resistance increase due to a drift angles is insignificant for the range found in normal service conditions with a constant heading while the other source of resistance increase, viz. due to rudder is to be taken into account for a tanker

$$\frac{\Delta R}{R} = 3.8\delta_R^2 \quad (4.5a)$$

and for a high speed cargo liner

$$\frac{\Delta R}{R} = 3.0\delta_R^2 \quad (4.5b)$$

with $\delta_R$ denoting the rudder angle in radian. The rudder and drift angles to balance a specified wind force can be obtained from $C_Y$ and $C_N$ data of wind tunnel test results /34 -36/.

If the wind is not constant with time, the ship is subject to yawing which can be another cause of resistance increase. Again according to Norrbin /39/, this is estimated by

for a tanker

$$\frac{\Delta R}{R} = 4.5\psi^2 \quad (4.6a)$$

and fof a high-speed cargo liner

$$\frac{\Delta R}{R} = 2.1\psi^2 \quad (4.6b)$$

The resistance increase due to rudder execution under yawing may be estimated by reducing the factors in equations (4.5a,b) to half, viz., 1.9 and 1.5.

## 4.2. Effect of Waves on Ship Resistance

Ship resistance increase in a seaway is estimated by either model resistance test in waves or theoretical calculation. Since it has been shown that the resistance increase is in proportion to the square of the wave height, the ship performance in any waves can be estimated by the plot of

$$\sigma_{AW} = \frac{R_{AW}}{\rho g h a (B/L)^2 L} \quad (4.7)$$

as a function of wave-length to ship-length ratio, wave direction, and Froude number.

Since Maruo's poineering work for development of linearized theory for resistance increase in waves /41/, many attempts have been made to adapt it for practical use and extend it to the calculations for oblique waves /42 - 45/. The agreement between them has reached a level of

'generally good', as shown in Figs.4.6 and 4.7 /46 - 47/ for those ships on which slender body theory assumption is acceptable.

For ships with blunt bow, effect of bow reflection should be considered as well as the resistance increase due to ship motion. Especially in relatively shorter wave length range, this contribution is large even though no discernible ship motions are observed. Fig.4.8 shows an example of components of resistance increase in waves.

On this problem there have been a number of investigations carried out and they report similar findings. Fujii and Takahashi /48/ introduced a semi-empirical formula based on the drifting force formula given by Havelock and showed that the bluntness coefficient is an improtant parameter on the aded resistance in shorter wave lengths. Kwon /49/ calculated the drift force by Bessho's formula for a cylinder with the same waterplane shape. The effect of finite draft was corrected by assuming an exponential decay of orbital motion with depth. Faltinsen et al. /50/ derived an asymptotic formula for shorter wave lengths from the momentum equation defined by the incident and the diffraction potentials. Fujii /50'/ showed that the expression for head waves, viz.,

$$R_{AW} = \frac{1}{2}\rho g h_A^2 \left(\sin^2\theta + \frac{2\omega_0 V_s}{g}\right) \qquad (4.8)$$

where $\theta$ = average waterline slope to the center line of the ship and
$\omega_0$ = circular frequency of the incident wave

give good agreement with the available experimental data.

Some typical examples of $R_{AW}$ are shown in Fig.4.9 for full ships with contribution of ship motions $R_{AW}(0)$ and that of bow reflection $R_{AW}(1)$ identified.

When the resistance increase in regular waves has been obtained by calculation or experiments, this can be extended to the value in irregular waves through

$$\overline{R_{AW}} = 2\int_0^\infty \frac{R_{AW}}{h_A^2}(\omega)\,[f(\omega)]^2 d\omega \qquad (4.9a)$$

or $$\overline{\sigma_{AW}} = 2\int_0^\infty \sigma_{AW}(\omega)\,[f(\omega)]^2 d\omega \qquad (4.9b)$$

for a given spectrum of the irregular waves.

According to the ITTC 1978 method, the total resistance coefficient is expressed with the hull wetted surface area with denominator. Therefore added resistance due to waves may be expresed by

$$C_T = C_F(1+K) + \Delta C_F + C_R + C_{AA} + C_{AW} \qquad (4.10)$$

where

$$C_{AW} = \frac{R_{AW}}{\frac{1}{2}\rho V_s^2 S}$$

$$\text{or} = \sigma_{AW}\frac{2gh_A^2B^2/L}{V_s^2 S}$$

Fig.4.10 is an example of this (but note that the $R_{AW}$ is divided by $\nabla^{2/3}$ instead of of S) correlating with the trial data of full ships /51/.

## 4.3. Effect of Waves on Open-Water Characteristics

In discussing the performance of a propeller in waves, effect of orbital velocities of the waves is to be primarily considered which causes fluctuations of the advance coefficient and corresponding fluctuations of the thrust and torque coefficients (Figs.4.11 and 4.12 /52/). To this end open-water tests in waves were carried out in several institutes. The results indicate, as illustrated in Figs.4.13 /52/ - 4.14 /53/ that time average thrust and torque coefficients are in good agreement with still water uniform flow characteristics. The fluctuating thrust and torque of the propeller operating below wave crests and troughs also agree with the still water characteristics when plotted to a base of the instantaneous advance coefficients calculated using the mean orbital velocities of the waves in way of the propeller disc from trochoidal wave theory.

Another factor to be considered is the effect of motion of a propeller due to ship motions in waves. This was investigated experimentally by forced oscillation of propeller boat which accommodated a propeller dynamometer. Of the three modes of oscillation---pitch, heave and surge---, fluctuations of thrust and torque appear in surging motion alone, except for the effect of weight of the propeller and its shafting appearing in pitching motion. The results

of the measurement made during the forced oscillation are shown in Figs.4.15, as well as the test set-up in Fig.4.16 /54/. From these figures it is evident that the mean thrust and torque of a surging propeller are almost the same as those when running steadily in open-water and that the fluctuating terms are in fairly good agreement with those calculated by a quasi-steady mothod.

These experimental results may be endorsed by the consideration for example when a propeller advances in waves of the reduced frequency $\frac{C\omega_0}{2V_s}$ is order of 1/100, and accordingly effect of unsteadiness is negligible when correction for unsteadiness is applied /53/.

### 4.4. Effect of Waves on Self-Propulsion Factors

Self-propulsion factors in waves are obtained by analysis of the results from the self-propulsion tests conducted in waves. Open-water characteristics of a propeller for analysis of wake fraction $W_M$ and relative rotative efficiency $\eta_R$ can be those in still water instead of those in waves, thanks to the conclusion described in the previous section 4.3. Figs. 4.17 - 4.18 ilustrate $W_M$ and $\eta_R$ thus analyzed for a cargo ship and a tanker /53/.

The data points scatter to a considerable extent due to the difficulty in the measurement in waves, but the mean lines can be regarded as those in still water.

For analysis of thrust deduction fraction, resistance data should be available in addition to the self-propulsion test results. Figs.4.19 - 4.21 are the results obtained from such pairs of tests /53, 54/, and from them it can be said that the mean line of the data points in waves can be taken as that in still water.

Looking at these figures closely it may be recognized that the wake fraction at the tuning point of ship's vertical motions $\lambda/L$ tends to be smaller (1-W larger). This may be interpreted as an effect of partial emergence of the propeller due to heavy ship motions. There is a proposal to explain this as a result from alteration of pressure distribution /50/ over the hull in waves and in motion, and this is correlated with the wake velocity measured by vane wheels /55/ on a model running in waves, but further investigation will be neccesary to identity this effect.

Summarizing, self-propulsion factors in waves can be regarded as equal to those in still water within the considerable band of resolution of measurements, unless the effects of propeller immersion are not critical.

## 5. ANALYSIS OF SERVICE PERFORMANCE-VOYAGE DATA

With the method and the materials presented above, it is possible to estimate the propulsive performance if the service conditions and the environmental conditions are known /57/. 'Possible' means a possibility in principle, but as a matter of course in some fields there are varied data and views among which it is difficult to choose a definitely recommendable one, or in others quantitative data are lacking as is the case with fouling effects.

Under such circumstances, needs for collecting more data and improving their reliability are evident, but it would be worth while to approach this through a different way, i.e. by analysis of service performance.

Those values which can be obtained by a log book are ship speed, rotational speed of the propeller and the factors corresponding to the output of the engine. These factors are different with the type of engine, of which the followings are commonly employed to estimate the power delivered to the propeller.

(1) Deisel Engine
- load indicator reading
- rpm of supercharger
- fuel oil consumption

(2) Steam Turbine
- first stage steam pressure
- fuel oil consumption

The quantities which can be read out of an abstract log book are such three values together with the environmental conditions during the navigation. This indicates that only two independent variables can be determined as a function of ship speed, although so many factors are involved in the service performance estimation (Fig.1.3) and analysis (Fig. 5.1). By properly processing the service

performance data, however, many factors can be analyzed if the environmental conditons are taken into account. Fig.5.2 is an example of daily data of power and rpm obtained from an abstract log book. Of them, only those data for the days of Beaufort scale equal to or less than 4 and propelling 24 hours will be extracted and reduced to mean values per voyage. For ships with specified mission such as tanker serving between Persian Gulf and Japan, the mean values per voyage are plotted to the time after entering service, for homeward (fully loaded) condition alone (Fig.5.3). These saw-tooth like curves can be divided into

(1) fouling effects which increase with the elapse of time after docking and
(2) ageing effects which, mostly due to deterioration of hull and propeller can not be recovered by docking

Fig.5.4 shows the fouling effect derived from Fig.5.3 /58/.

More generally, the load conditons are different with the voyage. This can be taken into account by analyzing the service performance data in terms of $\Delta C_{FC}$ and $\Delta W_C$. To do this, the resistance and propulsion test results are interpolated to match the actual service conditon, and open-water characteristics are estimated either considering surface deterioration or assuming them to be unchanged from those of the newly propeller. Fig.5.5 and 5.6 show examples obtained by Kawaguchi et al /59/. In this case, Hughes' friction line with form factor is used for $\Delta C_F$ and the full-scale wake fration is expressed by

$$e_i = \frac{1 - w_{TM}}{1 - w_{TS}} \qquad (5.1)$$

but this method can be applied to ITTC $\Delta C_{FC}$ and $\Delta W_C$ without any alteration of the principle.

Yamazaki analyzed further the resistance increase due to fouling in a similar manner, and showed that the results can be collapsed to a band of curves as shown in Fig.5.7 /60/, if the resistance increase is divided by average fouled surface area, in this case practically taken as that of side shells.

Effect of rough weather and seas can be analyzed from the difference of data between those less than Beaufort 4 (used in the analysis above) and those higher than that. An example of the analysis results is shown in Fig.5.8 /59/.

With the various factors obtained through the analyses mentioned above, service margin can be predicted in terms of power and rpm as a function of speed. Further, if ship motions and other factors critical of ship operation are incorporated, the prediction can be made on voluntary speed loss in rough seas. Recent studies indicate this possibility /60, 61/, of which a comparison of actual and predicted speeds (including both involuntary and voluntary speed loss) is in illustrated in Fig.5.9.

## 6. CONCLUDING REMARKS

In the above, it can be seen that practically all the aspects concerning service performance prediction and analysis have been covered by many investigations carried out up to the present. Thanks to those, it is now possible to apply the ITTC 1978 analytical method to service performance problems to quantify a number of factors involved in them.

At the same time, the reader may have noted lack of data and reliability in many respects. These should be supplemented by model experiments and full-scale measurement.

It is hoped therefore that the contributions from both ship builders' and ship owners' sides are directed to a common objective i.e. economical operation of ships based on scientific considerations.

## References


1. Taniguchi, K.: "Model-ship Correlation Method in the Mitsubishi Experimental Tank", Mitsubishi Technical Bulletin No.12 (1963), Journal of Soc. Nav. Arch. of Japan, Vol.113 (1964).
2. Lindgren, H. and Dyne, G.: "Ship Performance Prediction", International Sumposium on Advances in Marine Technology, Trondheim, Proceedings Vol.1 (1979).
3. Brard, R. and Aucher, M.: "Resistance a la Marche, Rillage, Succion Effect d'Echelle sur la Propulsion", Trans. ATMA, (1969).
4. "1978 ITTC Performance Prediction Method for Single Screw Ships", Report of Performance Committee, Proc. of ITTC 78 pp.388-404 (1978).

5. Hacking, H.: "B.S.R.A. Method of Measuring and Analyzing Hull Surface Roughness", Proc. of the International Ship Painting and Corrosion Conference, London, (1974).
6. Parker, M.: "Assessing Surface Deterioration", The Motor Ship, April (1978).
7. Bowden, B.S. and Davison, N.J.: "Ship Resistance and Hull Roughness", NPL Ship TM 356, July (1973).
8. Bowden, B.S. and Davison, N.J.: "Resistance Increments due to Hull Roughness Associated with Form Factor Extrapolation Method", NPL Ship TM 380, January (1974).
9. Nikuradse, J., "Stroemungsgesetze in rauhen Rohren, Forschg.-arb. Ing.-Wesen No.361 (1933).
10. Prandtl, H, and Schlichting, H.: "Das Widerstandsgesetz rauher Platten, Werft", Reederei, Hafen (1934).
11. Muntjewerf, J.J. and Bowden, B.S.: "Hull Deterioration and Fouling", 14th ITTC Report of Performance Committee Appendix 7 (1975).
12. Karlsson, R.I.: "The Effect of Irregular Surface Roughness on the Frictional Resistance of Ships", Symp. on Ship Viscous Resistance, Goteborg (1978).
13. Musker, A.J. and Lewkowicz, A.K.: "The Effect of Ship Roughness on the Development of Turbulent Boundary Layers", Do. (1978).
14. Yamazaki, Y., Onogi, H., Nakato, M., Mimino, Y., Tanaka, I. and Suzuki, T.: "Resistance Increase due to Surface Roughness (1st Report)", Journal of Soc. Naval Architects of Japan, Vol.153 (1983).
15. Tokunaga, K. and Baba, E.: "Approximate Calculation of Ship Frictional Resistance Increase due to Surface Roughness", Journal of Soc. Nav. Arch. Japan, Vol.152 (1983).
16. Townsin, R.L., Byrne, D., Milne, A. and Svenson, T.: "Speed, Power and Roughness: The Economics of Outer Bottom Maintenance", Trans. RINA, Vol.122 (1980).
17. Clauser, F.H.: "The Turbulent Boundary Layer", Advances in Applied Mechanics, Vol.4 (1956).
18. Sasajima, H. and Himeno, Y.: "Scale Correction for Roughness Effect", Journal of Soc. of Nav. Arch. Japan, Vol.118 (1965).
19. Burnett, R.F.: "The Smooth Hull's Contribution to Fuel Saving", Shipbuilding & Marine Engineering International, October (1982).
20. Grigson, C.W.B.: "The Drag Coefficients of a Range of Ship Surface II", Trans. RINA (1982).
21. Tokunaga, K. and Baba, E.: "A Study on Local Roughness Effect on Ship Resistance", Trans. West Japan Soc. Nav. Arch. No.59 (1980).
22. Lerbs, H.W.: "On the Effect of Scale and Roughness on Free Running Propellers", Journal of American Society of Naval Engineers, No.1 (1951).
23. Meyne, K.: "Einfluss der Oberflaechenrauhigkeit auf die Leistungsaufnahme von Propellers", Jahrbuch STG Band 76 (1982).
24. Contribution of Nagasaki Experimental Tank to Design of Hull Form and Propeller, Part III "Study on Propeller and Cavitation for Design of Propellers", 75th Anniversary (1983).
25. Yokoo, K. et al: "Effect of Fouling of Ship's Hull and Propeller upon Propulsive Performance", Report of Transportation Technical Research Institute, No.22 Sept. (1956).
26. Emerson, A.: "Roughness and Scale Effect on Propellers", Int. Shipbuilding Progress, Vol.5. No.43, (1958).
27. Ferguson, J.M.: "The Effect of Surface Roughness on the Performance of a Model Propeller", Trans., INA., Vol.100, (1958).
28. Byrne, D., Fitzsimmons, P.A. and Brook, A.K.: "Maintaining Propeller Smoothness: A Cost Effective Means of Energy Saving", SNAME Combined Symposium on Ship Costs and Energy, New York, (1982).
29. Hundley, L.L.: "The Effects of Fouling on the Powering Characteristics of U.S. Navy Surface Combatants", 19th ATTC Ann Arbor (1980).
30. Tanibayashi, H.: "Cavitation of Marine Propellers", Proc. 2nd Symp. on Marine Propellers, Soc. Nav. Arch. Japan (1981).
31. Gawn, R.W.L.: "Roughened Hull Surface", Trans. NECIS., Vol.58 (1942).

Harvald, Sv. Aa. and Hee, Jan M.: "Wake Distributions", 75 Jahre VWS Berlin (1978).
Tokunaga, K.: "Local Roughness Effect on Self-Propulsion Factors", Trans. West Japan Soc. Nav. Arch. No.63 (1982).
Isherwood, R.M.: "Wind Resistance of Merchant Ships", Trans. RINA, Vol.115 (1973).
Wagner, B.: "Windkraefte an Ueberwasserschiffen", Jahrbuch STG, (1967).
Van Berelkom, W.X: "Traegarden, P. and Dellhag, A.: "Large Tankers-Wind Coefficients and Speed Loss Due to Wind and Sea", Trans. RINA (1974).
Tsuji, T., Takaishi, T., Kan, M., Sato, T.: Model Experiments on Wind Forces of Ships, Report of Ship Research Institute, Japan, Vol.7, No.5 (1970).
"JTTC Tentative Standard for analysis of Speed Trial Results", Bulletin Soc. Nav. Arch. Japan (1944).
Wilson, C.J. and Roddy, R.F.: "Estimating the Wind Resistance of Cargo ships and Tankers", NSRDC Rep.3355 (1970).
Norrbin, N.H.: "On the Added Resistance due to Steering on a Straight Course", Appendix 8 to Report of 13th ITTC Performance Committee, (1972).
Maruo, H.: "Resistance in Waves, Research or Seakeeping Qualities of Ship in Waves", Journal Soc. Nav. Arch. Japan, 60th Anniversary Series, Vol.8, Chap.5 (1963).
Gerritsma, J. and Beukelman, W.: "Analyses of the Resistance Increase in Waves of a Fast Cargo Ship", Appendix 5 of Report Seakeeping Committee, Proc. 13th ITTC, Vol.2 (1972).
Strom-Tejsen, J., Yeh, H.Y.H. and Moran, D.D.: "Added Resistance in Waves", Trans. SNAME, Vol.81 (1973).
Hosoda, R.: "The Added Resistance of Ships in Regular Oblique Waves", Journal Soc. Nav. Arch. Japan, Vol.133 (1973).
Yamazaki, R.: Nakatake, I., Kino, S. and Koguchi, K.: "On the Propulsive Performance of a Ship in Regular Head Waves, Journal Soc. Nav. Arch. Japan, Vol.143 (1978).
46. Nakamura, S. and Fujii, H.: "Nominal Speed Loss of Ships in Waves", PRADS-International Symposium on Practical Design in Shipbuilding, Tokyo, (1977).
47. Shintani, A and Yamazaki, Y.: "Propulsion Test on a Ship Model in Waves, Symposium on Ship Model Testing, Soc. Nav. Arch. Japan, Tokyo (1983).
48. Fujii, H. and Takahashi, T.: "Experimental Study on the Resistance Increase of a Large Full Ships", Journal Soc. Nav. Arch. Japan, Vol.137 (1975), and Proc. 14th ITTC Vol.4 (1975).
49. Kwon, Y.J.: "The Effect of Weather, Particularly Short Sea Waves, on Ship Speed Performance". Ph.D. Thesis, University of Newcastle upon Tyne (1982).
50. Faltinsen, O.M., Minsaas, K.J., Liapis, N. and Skjordal, S.O.: "Prediction of Resistance and Propulsion of Ship in Seaway", Proc. 13th Symp. on Naval Hydrodynamics, Tokyo, (1980).
50'. Fujii, H. Discussion to Reb-50.
51. Takahashi, T. and Tsukamoto, S.: "Effect of Waves on the Results of Speed Trial of Large Full Ships", Trans. West Japan Soc. Nav. Arch. No.54 (1977).
52. McCarthy, J., Norley, W.H. and Ober, G.L.: "The Performance of a Fully Submerged Propeller in Regular Waves", DTMB Report 1440, May 1961.
53. Taniguchi, K., "Propulsive Performance of Ships in Waves, Bulletin Soc. of Nav. Arch. Japan, No.383, (1961).
54. Nakamura, S., Naito, S. and Inoue, R.: "Open-Water Characteristics and Load Fluctuations of Propeller in Waves", Journal Kansai Soc. Nav. Arch. Japan, No.159, (1975).
55. Nakamura, S., Hosoda, R., Naito, S. and Inoue, M.: "Propulsive Performance of a Container Ship in Waves (4th Report)", Journal Kansai Soc. Nav. Arch. Japan, No.159, (1975).
56. Moor, D.I. and Murdey, D.C.: "Motions and Propulsion of Single Screw Models in Head Seas, Part II", Trans. RINA Vol.112 (1970).
57. Prediction of Service Margin, Report of the Performance Committee ITTC 81 Leningrad (1981).

58. Tanaka, M. and Mizoguchi, S.: "Computer Program for Analyzing Voyage Data and an Example of Analysis", IHI Engineering Review, Vol.14, No.4, (1981).

59. Kawaguchi, N., Takekuma, K., Hashiguchi, K., Ise, T. and Shimizu, T.: "On a New Analyzing Method of Ship's Service Performance", Journal Kansai Soc. Nav. Arch. Japan, No.152 (1974).

60. Yamazaki, Y. and Sakamoto, M.: "On the Service Speed", Journal Soc. Nav. Arch. Japan, Vol.146 (1979).

61. Schenzle, P.: "Leistungsbedarf und Schiffsgeschwindigkeit unter Dienstbedingungen", Jahrbuch STG Band 73 (1979).

Nomenclature

$A_0, A_1, A_2, A_3$ Coefficients for Isherwood's formula for estimation of wind resistance coefficient
$A_T$ Transverse area of above-water part of a ship
B Breadth of a ship
C Chord length of a propeller
$C_{AA}$ Wind resistance coefficient $R_{AA}/\frac{1}{2}\rho V_S^2 S$
$C_{AW}$ Non-dimensional resistance increase in waves $R_{AW}/\frac{1}{2}\rho V_S^2 S$
$C_F$ Frictional coefficient
$\Delta C_F$ Roughness allowance for $C_F$
$\Delta C_{FC}$ Model-ship correlation factor applied to $(C_F + \Delta C_F)$, cf. Table 1
$\delta\Delta C_F$ Increase of $\Delta C_F$ under service condition
$C_N$ Model-ship correlation factor for number of revolutions of a propeller, cf. Table 1
$C_{NP}$ Do. Based on power identity, cf. Table 1
$C_P$ Model-ship correlation for delivered horsepower, cf. Table 1
$C_R$ Residual resistance coefficient
$C_{TS}$ Total resistance coefficient of a ship
$C_X$ Wind resistance coefficient relating to $A_T$, $R_{AA}/\frac{1}{2}\rho_{air} V_R^2 A_T$
D Diameter of a propeller
$D_E$ Number of extreme values
$D_Z$ Number of zero-crossings
$e_i$ Model-ship correlation factor for wake fraction
Fn Froude number
g Acceleration of gravity
J Advance coefficient of a propeller
ha Wave amplitude
$h_+$ Mean value of peak-to-trough roughness height
K Karman's constant for boundary layer flow
$K_T$ Thrust coefficient of a propeller
$K_Q$ Torque coefficient of a propeller
k Form factor relating to frictional resistance of a ship, Nikuradse's sand roughness, Wind direction coefficient, $C_X(\theta)/C_X(0)$
$k_p$ Roughness of a propeller blade
$k_s$ Roughness of a hull Niduradse's sand roughness (Figs.3.2 and 3.3)
L Length of a ship
$L_{WL}$ Length of water line
M Suffix indicating model values
m Roughness texture parameter according to Grigson
$m_0$, $m_2$, $m_4$ Moments of roughness profile
$n_S$ Number of revolutions of a propeller
$n_T$ Do. for trial condition
P Pitch of a propeller
$P_{DS}$ Delivered horse-power
$P_{DT}$ Do. for trial condition
$R_{AW}$ Resistance increase in waves
$R_n$ Reynolds number
S Wetted surface area of a ship
Suffix indicating full-scale values
t Roughness texture parameter
Thrust deduction fraction
u Velocity in the direction of general flow
$u_0$ Shear velocity, $\sqrt{\tau/\rho}$
$\Delta_u$ Velocity defect due to roughness in a boundary layer
$V_R$ Wind speed relative to ship
$V_S$ Ship speed
$W_T$ Taylor's wake fraction
$\Delta W_C$ Model-ship correlation for wake fraction
Z Number of propeller blades
$\bar{\alpha}$ Roughness texture parameter
$\delta_R$ Rudder angle
$\zeta_a$ Wave amplitude, ha
$\eta_R$ Relative rotative efficiency
$\theta$ Angle of incidence of wind
$\lambda$ Wave length
$\mu$ Direction of incident waves
$\nu$ Kinematic viscosity of a fluid
$\rho$ Density of water
$\rho_a$ Density of air
$\sigma_{AW}$ Non-dimensional resistance increase in waves, $R_{AW}/\rho gha(L^2/B)$
$\tau$ Wall-shear stress of turbulent flow
$\Psi$ Yawing amplitude
$\omega_0$ Circular frequency of incident wave

Table 1 ITTC 1978 Performance Prediction Method

(1) $V_S$ (m/s) given

(2) $R_e = \frac{V_S L_{WLs}}{\nu}$

(3) $F_n = V_S / \sqrt{g L_{WLs}}$

(4) $C_R$ from resistance test results

(5) $k$ do.

(6) $C_{FS} = \frac{0.075}{(\log Re - 2)^2}$

(7) $\Delta C_F = \{ 105 (k_s/L)^{1/3} - 0.64 \} \times 10^{-3}$ with $k_s = 150 \times 10^{-6}$m

(8) $C_{AA} = 0.001 A_T/S$

(9) $C_{TS} = (1+K) C_{FS} + \Delta C_F + C_R + C_{AA}$

(10) $t$ }
(11) $W_{TM}$ } from propulsion test results
(12) $\eta_R$ }

(13) $W_{TS} = (t + 0.04) + (W_{TM} - t - 0.04) \times \frac{(1+k) \cdot C_{FS} + \Delta C_F}{(1+k) C_{FM}}$

(14) $\frac{K_T}{J^2} = \frac{S}{2D^2} \cdot \frac{C_{TS}}{(1-t) \cdot (1-W_{TS})^2}$

(15) $J_{TS}$ from the open-water characteristics of the full scale propeller

(16) $K_{QTS}$ do.

(a) $C_P - C_N$ corrections

(17) $n_s = \frac{(1-W_{TS}) \cdot V_S}{J_{TS} \cdot D}$ (rps)

(18) $n_T = C_N \cdot n_s$ (rps)

(19) $P_{DS} = 2\pi\rho D^5 n_s^3 \frac{K_{QTS}}{\eta_R} \cdot 10^{-3}$ (kw)

(20) $P_{DT} = C_P \cdot P_{DS}$ (kw)

(b) $\Delta C_{FC} - \Delta W_C$ corrections

(14)' $\frac{K_T}{J^2} = \frac{S}{D^2} \cdot \frac{C_{TS} + \Delta C_{FC}}{(1-t)(1-W_{TS}-\Delta W_C)^2}$

(15) (16) the same as above

(18)' $n_T = \frac{(1-W_{TS}-\Delta W_C) \cdot V_S}{J_{TS} \cdot D}$ (rps)

(20)' $P_{DT} = 2\pi\rho D^5 n_T^3 \frac{K_{QTS}}{\eta_R} 10^{-3}$ (kw)

(c) $C_P - C_{NP}$ corrections

(17) (20) the same as above

(21)" $\left(\frac{K_Q}{J^3}\right)_T = \frac{1000 C_P P D_S}{2\pi\rho D^2 V_S^3 (1-W_{TS})^3}$

(22)" $\frac{K_{Q0}}{J^3} = \left(\frac{K_Q}{J^3}\right)_T \cdot \eta_R$

(23)" $J_{TS}$

(24) $n_s = \frac{V_S(1-W_{TS})}{J_{TS} \cdot D}$

(25) $P_{DT} = C_P \cdot P_{DS}$ (kw)

(26) $n_T = C_{NP} \cdot n_s$ (rps)

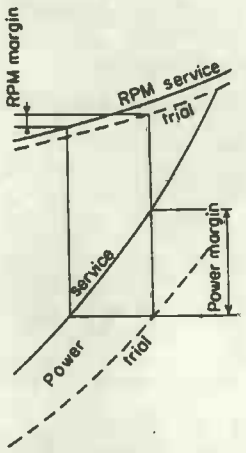


Fig.1.1 Power and RPM Curves under Trial and Service Conditions

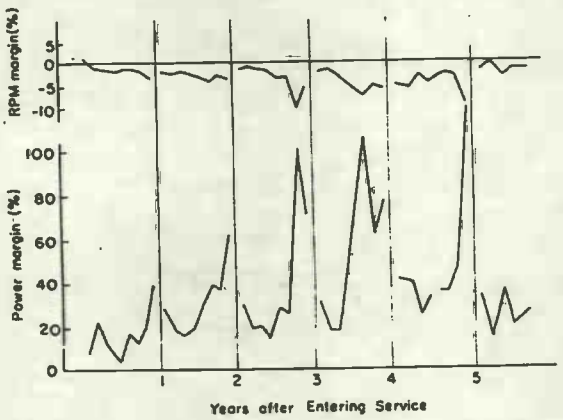


Fig.1.2 Example of Power and RPM Margins after Entering Service

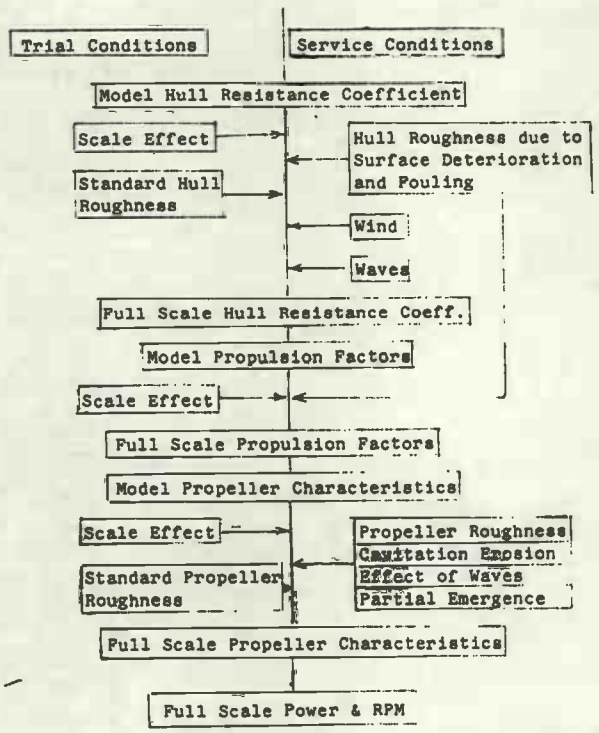


Fig.1.3 Prediction of Propulsive Performance under Trial and Service Conditions

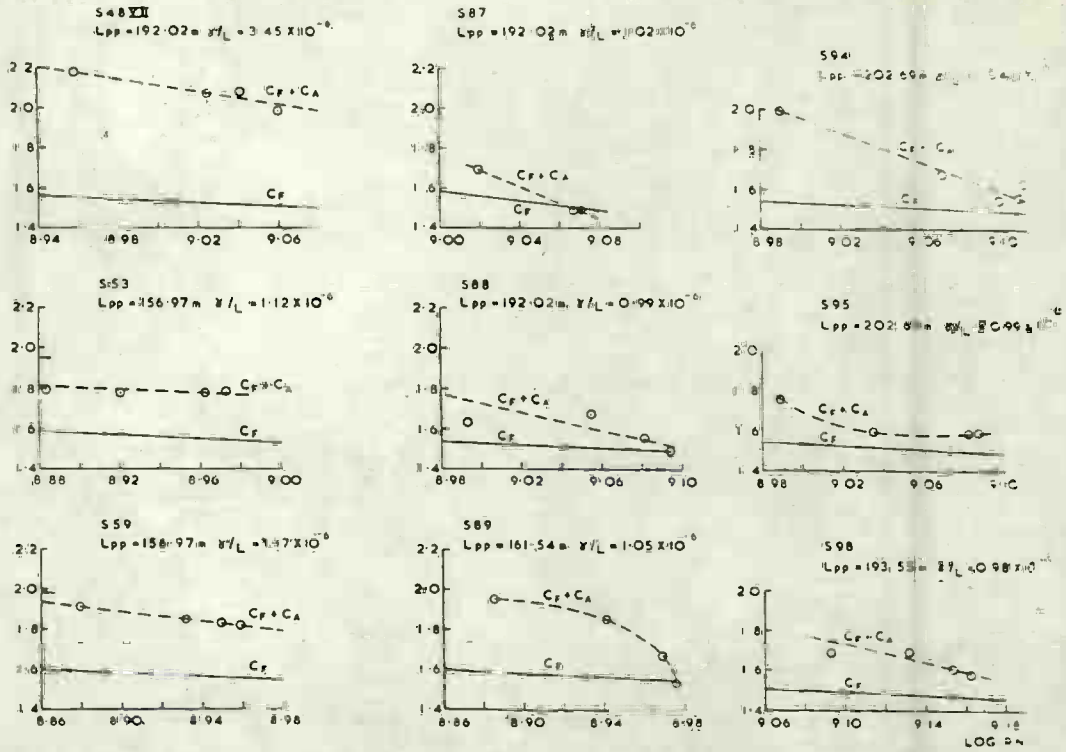


Fig.3.1 Full-Scale ( $C_F + \Delta C_F$ ) Values Derived from Thrust Measurements /7/

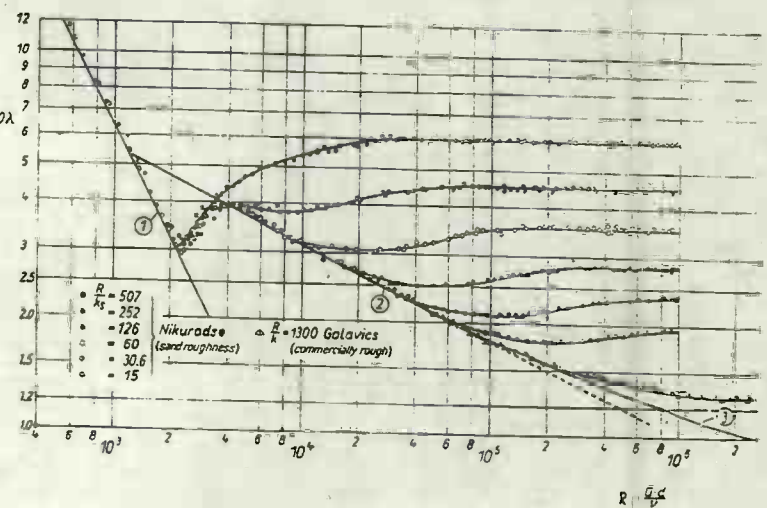


Fig. 3.2
Resistance Coefficients for Rough Pipes /10/

$$\frac{p_1 - p_2}{L} = \frac{\lambda}{d}\,\frac{1}{2}\,\rho\,\bar{u}^2$$

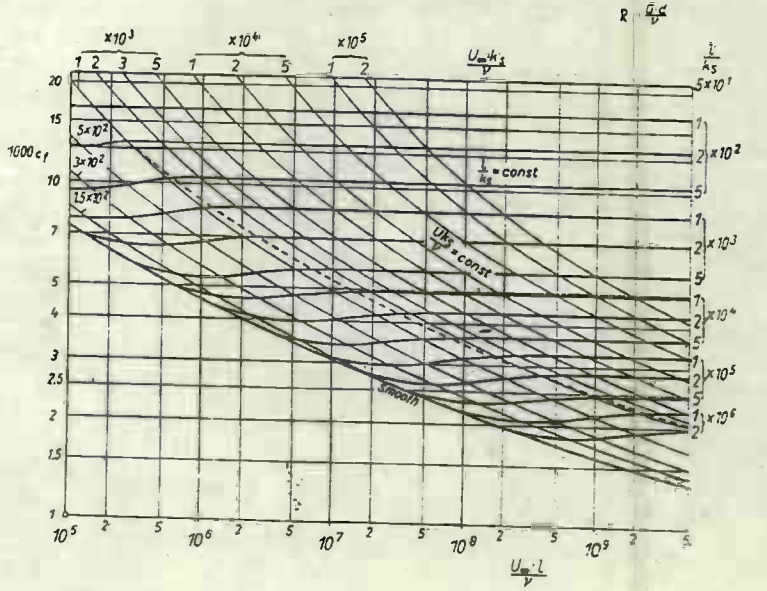


Fig. 3.3
Resistance Coefficients of Sand-Roughened Plates /10/

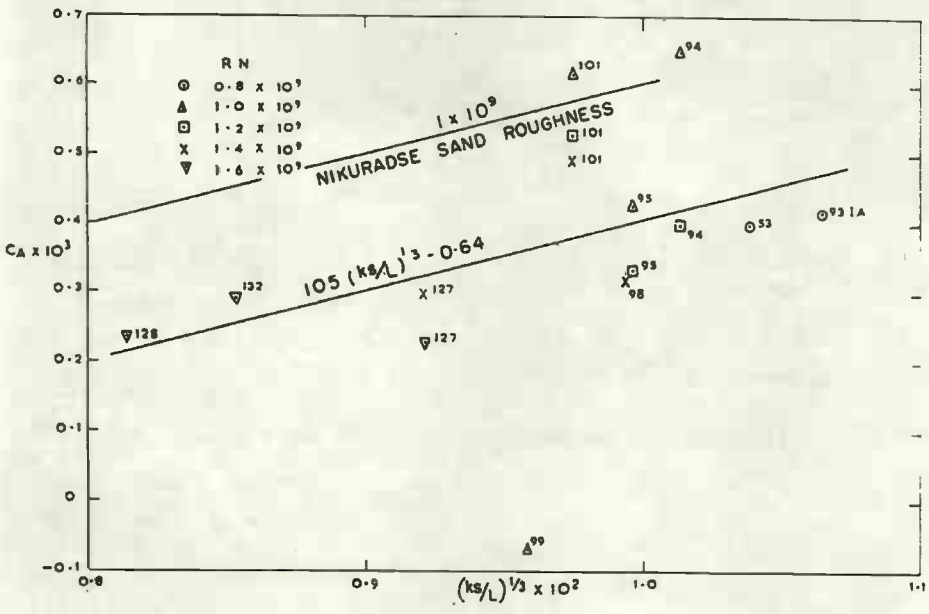


Fig.3.4 $\Delta C_F$ ( = $C_A$ ) as a Function of Hull Roughness / Length Ratio /8/

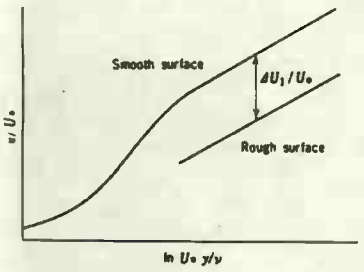


Fig.3.5 Example of Roughness Functions /14/

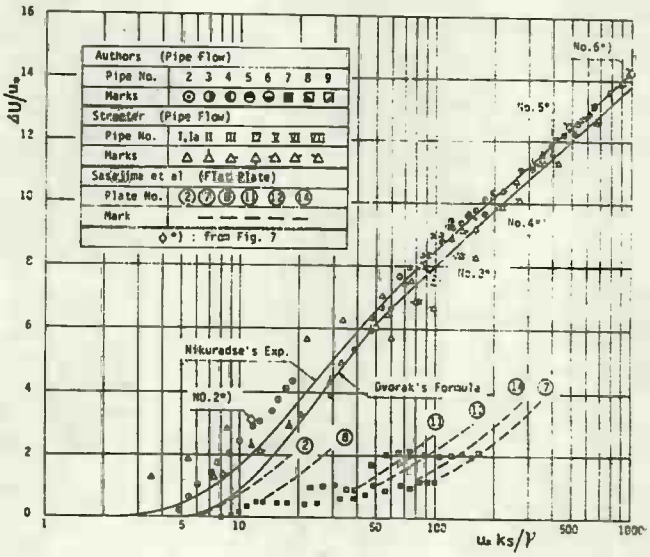


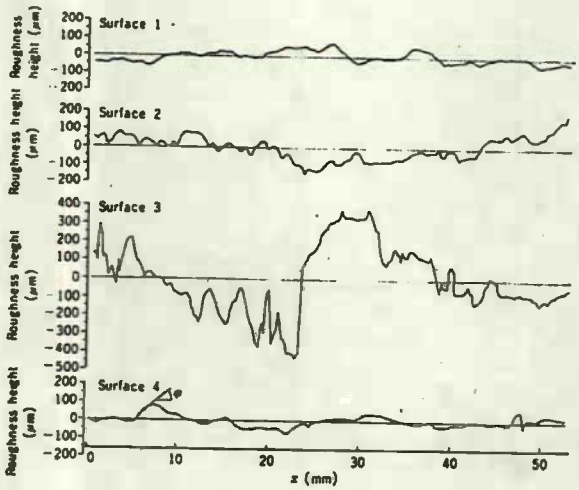


Analytical description and extrapolation of measured roughness functions for rough surfaces No. 1~4[8]

| | |
|---|---|
| Surface 1 : $\sigma_y$ = 31 μm | Surface 2 : $\sigma_y$ = 65 μm |
| $\frac{\Delta U_1}{U_\tau}$ = 0 ; $0 \le R_k \le 3.05$, | $\frac{\Delta U_1}{U_\tau}$ = 0 ; $0 \le R_k \le 3.8$, |
| $\frac{\Delta U_1}{U_\tau}$ = 0.6($R_k$ − 3.05) ; $3.05 < R_k \le 5.7$, | $\frac{\Delta U_1}{U_\tau}$ = 0.35($R_k$ − 3.8) ; $3.8 < R_k \le 10$, |
| $\frac{\Delta U_1}{U_\tau}$ = 2.44 ln $R_k$ − 2.65 ; $R_k > 5.7$. | $\frac{\Delta U_1}{U_\tau}$ = 2.44 ln $R_k$ − 3.45 ; $R_k > 10$. |
| Surface 3 : $\sigma_y$ = 183 μm | Surface 4 : $\sigma_y$ = 29 μm |
| $\frac{\Delta U_1}{U_\tau}$ = 0 ; $0 \le R_k \le 6.6$, | $\frac{\Delta U_1}{U_\tau}$ = 0 ; $0 \le R_k \le 3.3$, |
| $\frac{\Delta U_1}{U_\tau}$ = 0.6($R_k$ − 6.6) ; $6.6 < R_k \le 9.0$, | $\frac{\Delta U_1}{U_\tau}$ = 0.6($R_k$ − 3.3) ; $3.3 < R_k \le 6.0$, |
| $\frac{\Delta U_1}{U_\tau}$ = 3.8 ln $R_k$ − 6.9 ; $9.0 < R_k \le 17$, | $\frac{\Delta U_1}{U_\tau}$ = 2.44 ln $R_k$ − 2.75 ; $R_k > 6.0$. |
| $\frac{\Delta U_1}{U_\tau}$ = 2.44 ln $R_k$ − 3.05 ; $R_k > 17$. | |

Fig. 3.6 Surface Profile and Roughness Function Obtained by Wind Tunnel Experiments /12/

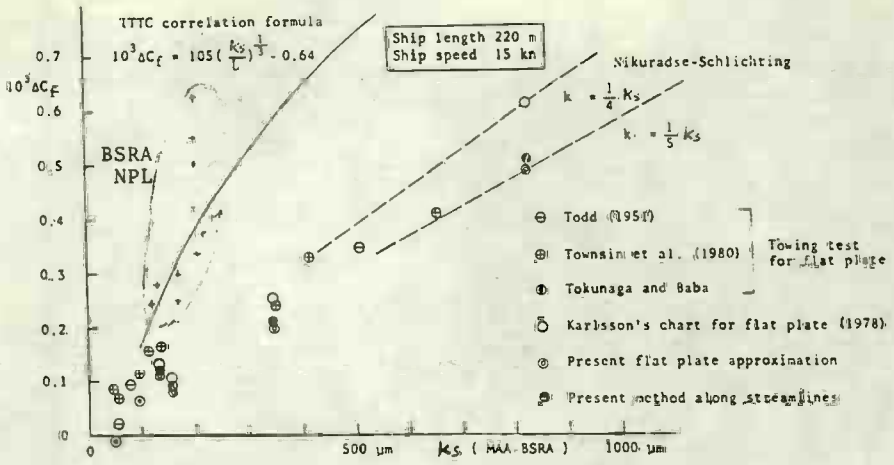


Fig.3.7 Relationship between $C_F$ and Roughness Height /15/

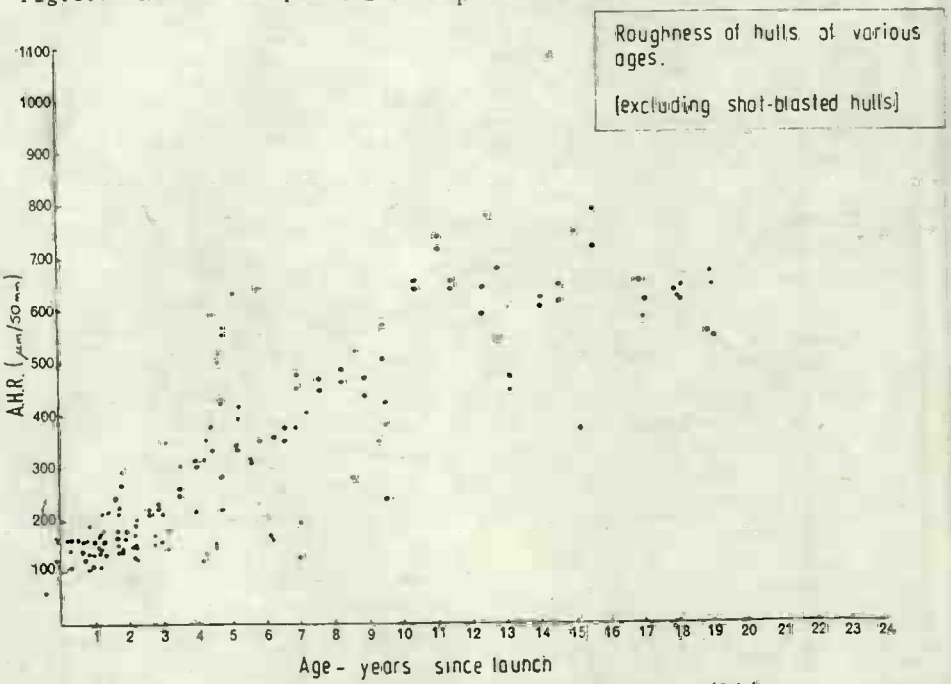


Fig.3.8 Average Hull-Roughness of Various Ages /16/

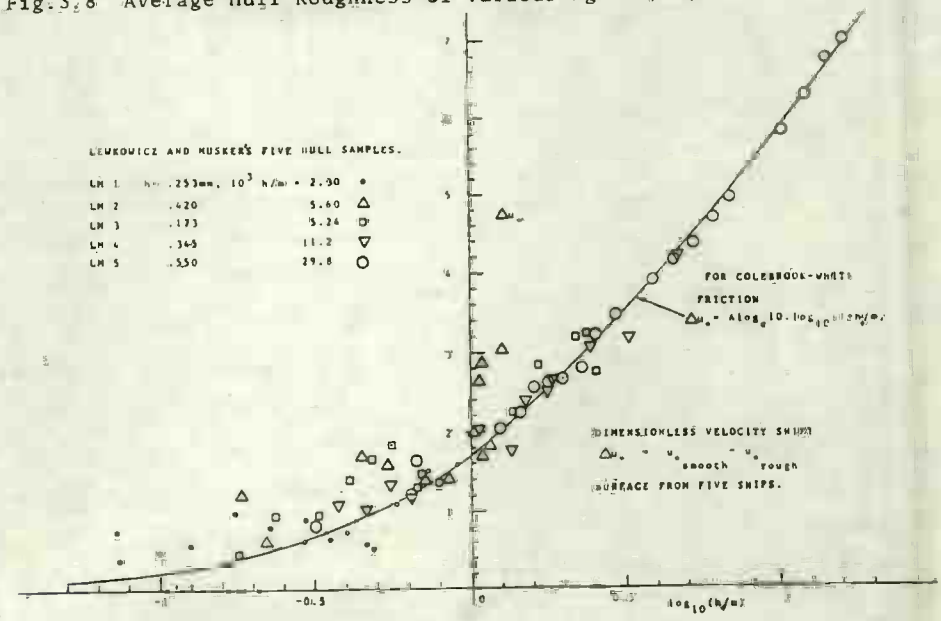


Fig.3.9 Universal Roughness Function Derived by Grigson /20/


Fig.3.10 Example of Slime Growing on a Ship Model /21/

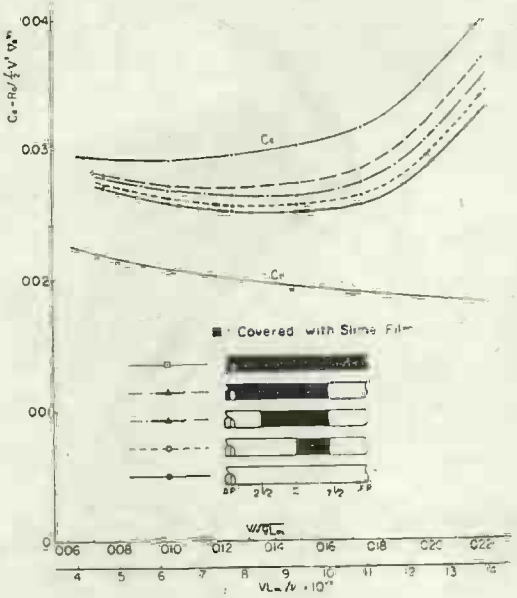


Fig.3.11 Effect of Hull Roughness and its Locations on Resistance Test Results /21/

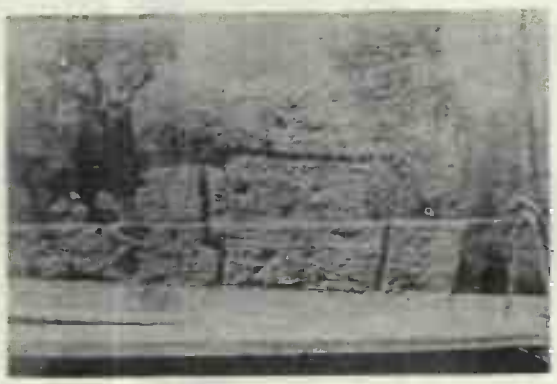

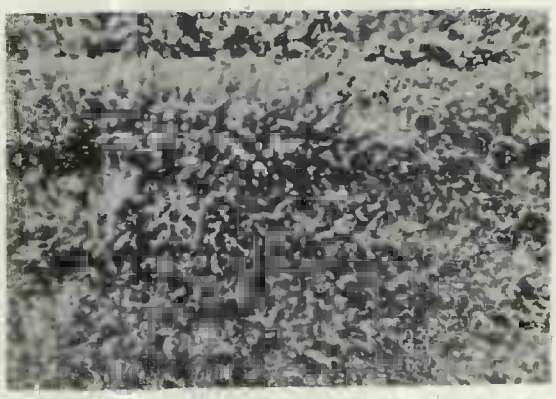

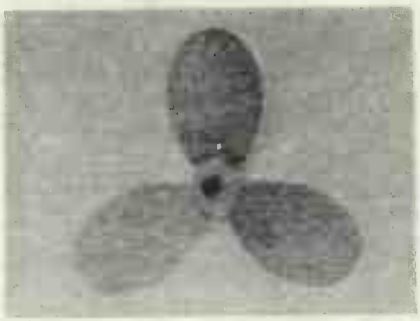

Fig.3.12 Example of Marine Growth on Hull and Propeller

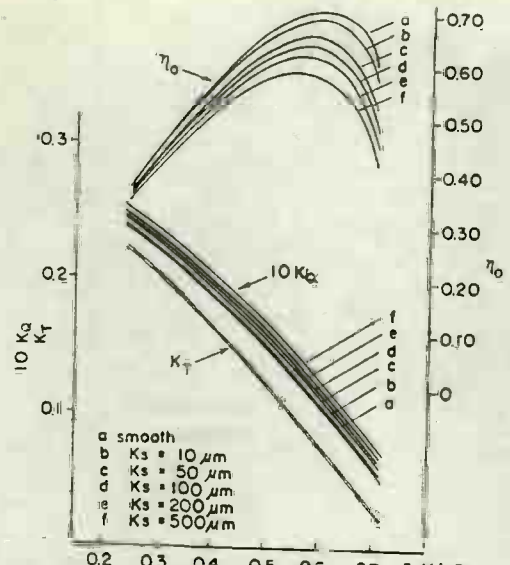


Fig.3.13 Sample Calculation of Roughness Effect on Open-Water Characteristics of Propeller /23/

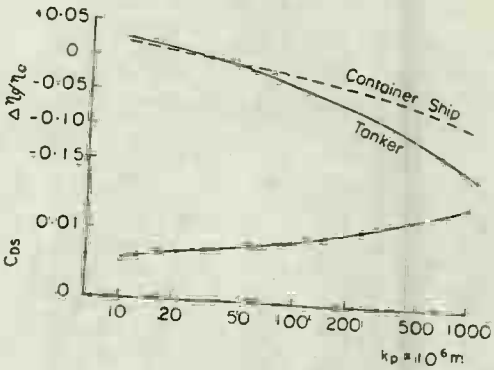


Fig.3.14 Sample Calculation of Roughness Effect on Propeller Efficiency

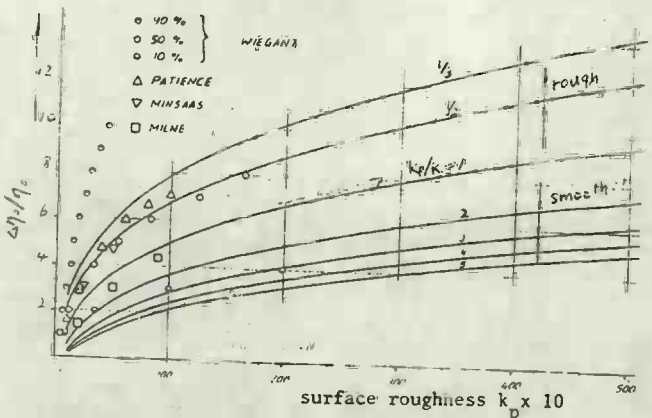


Fig.3.15 Roughness Effect on Propeller Efficiency /23/

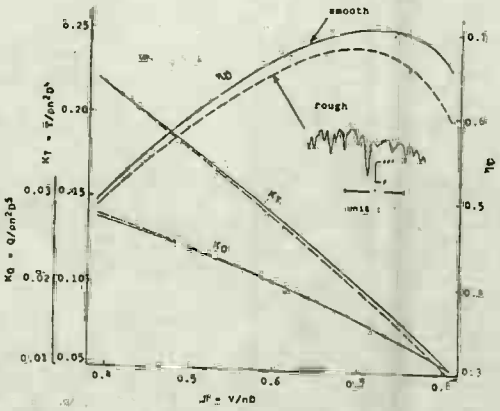


Fig.3.16 Results from Model Experiments on a Roughened Propeller (1) /24/

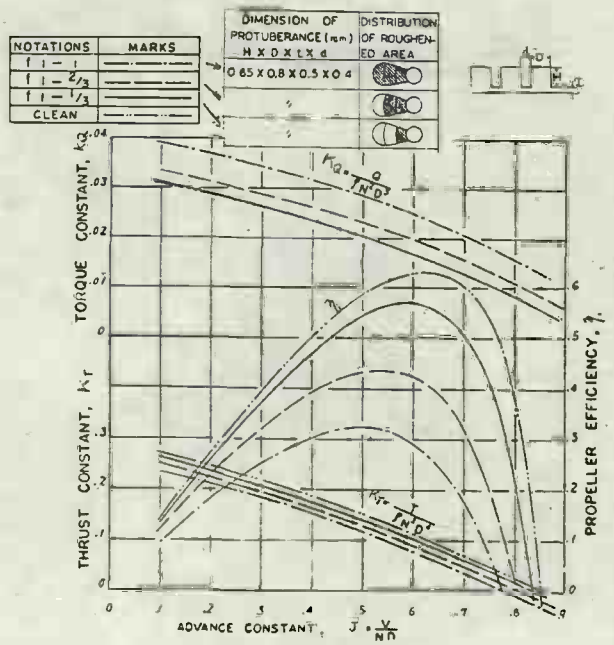


Fig.3.17 Results from Model Experiments on a Roughened Propeller (2) /25/

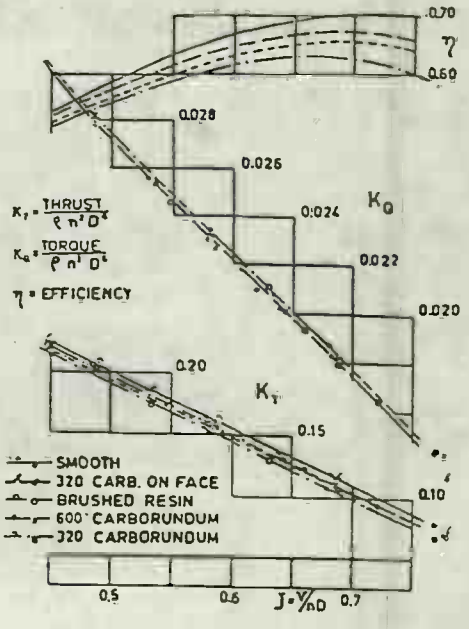


Fig.3.18 Results from Model Experiments on a Roughened Propeller (3) /26/

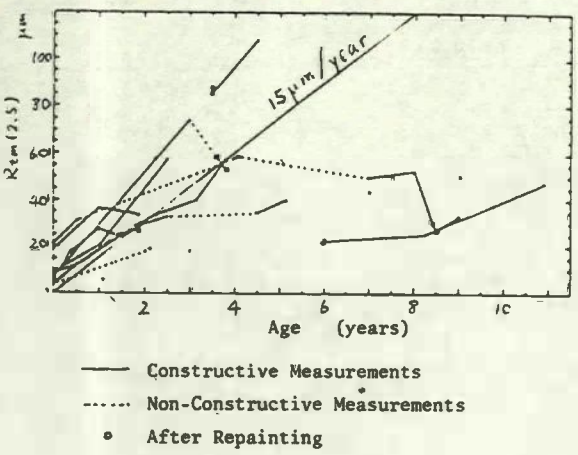


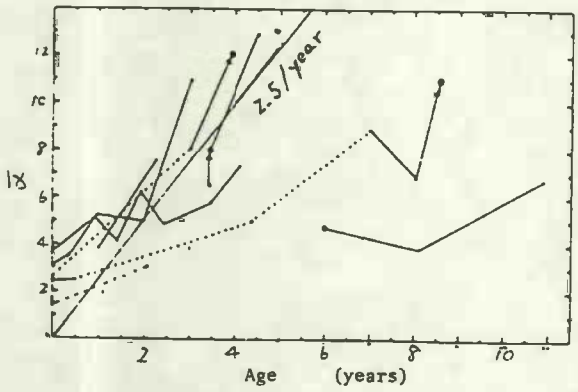


Fig.3.19 Propeller Surface Roughness of Various Ages /28/

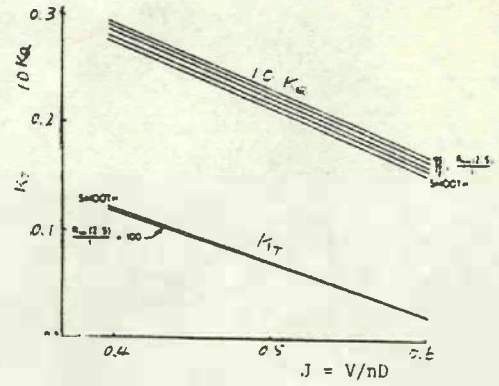


Fig.3.20 Propeller Roughness Effect Calculated as a Function of $R_{tm}/t$ /28/

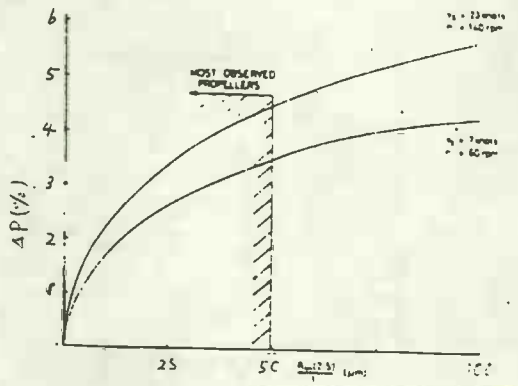


Fig.3.21 Sample Calculation of Power Increase as a Function of $R_{tm}/t$ /28/

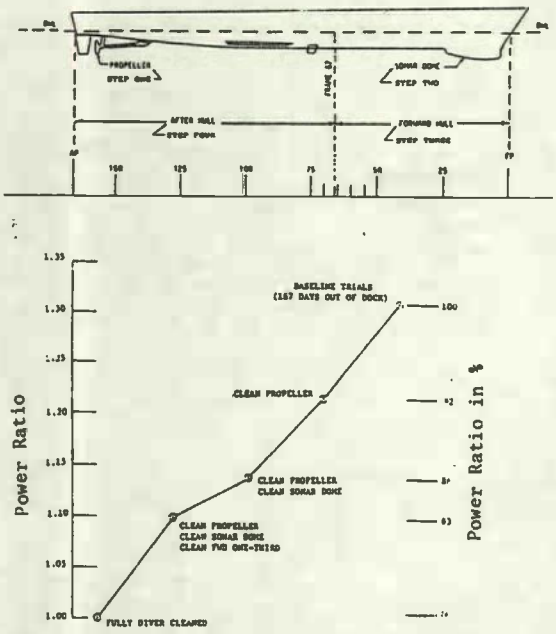


Fig.3.22 Variation of Power with Cleaning of Various Parts of a Ship /29/

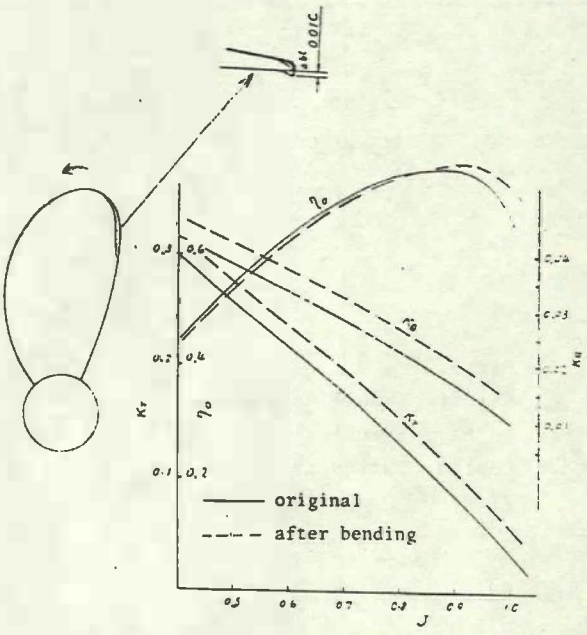


Fig.3.23 Effect of Bent Trailing Edge on Propeller Characteristcs /30/

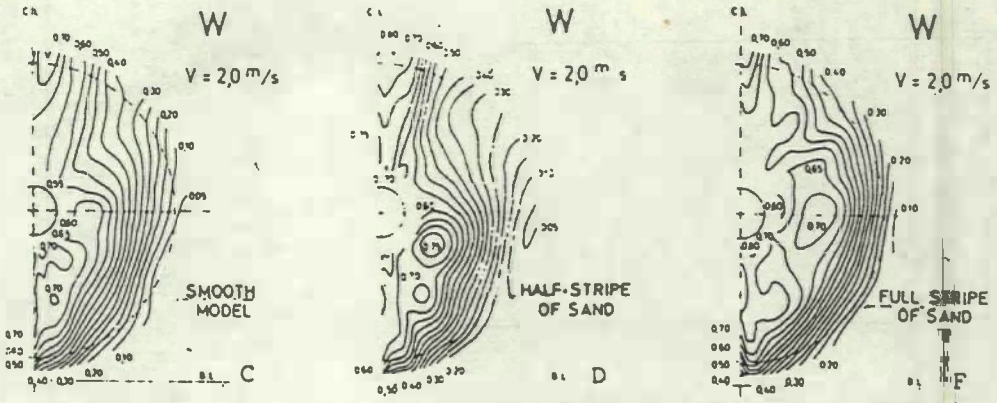


Fig.3.24 Effect of Hull Roughness on Wake Fraction Contours in the Plane of Propeller /32/

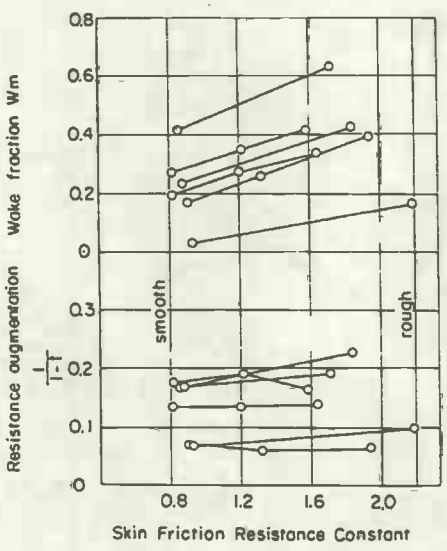


Fig.3.25 Effect of Hull Roughness on Self-Propulsion Factors (1) /31/

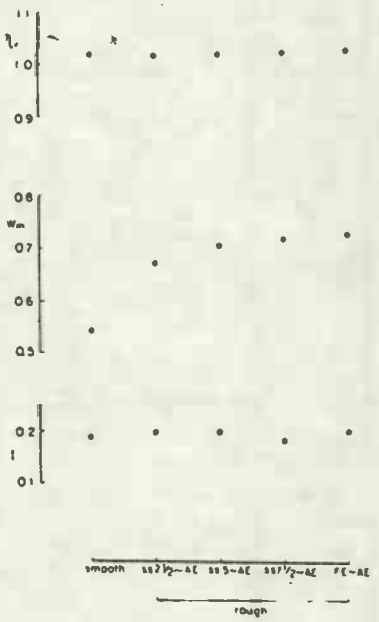


Fig.3.26 Effect of Hull Roughness on Self-Propulsion Factors (2) /32/

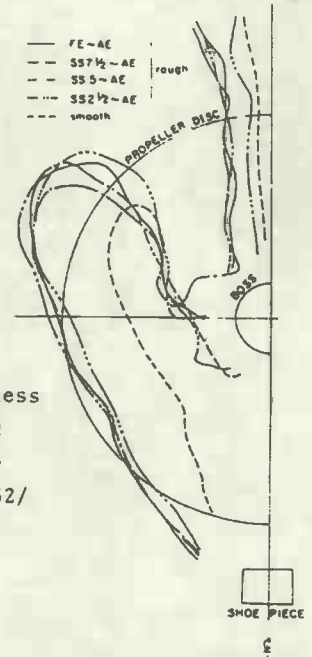


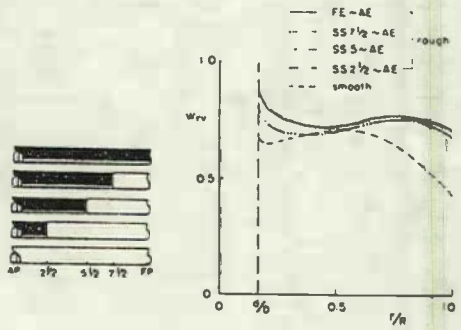


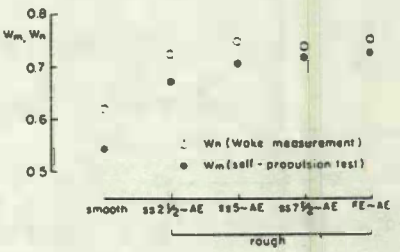


Fig.3.27
Effect of Hull Roughness on Wake Fractions and Contour Curves in the Plane of Propeller /32/

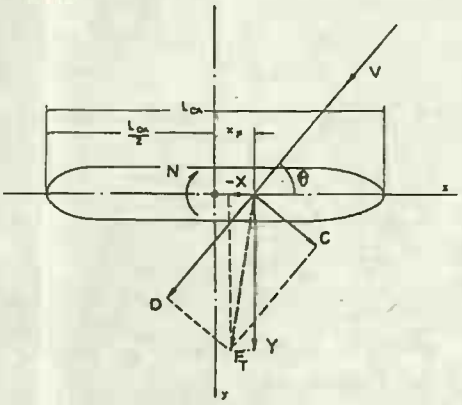


Fig.4.1 Wind Forces and Moments Measured by Wind Tunnel Tests

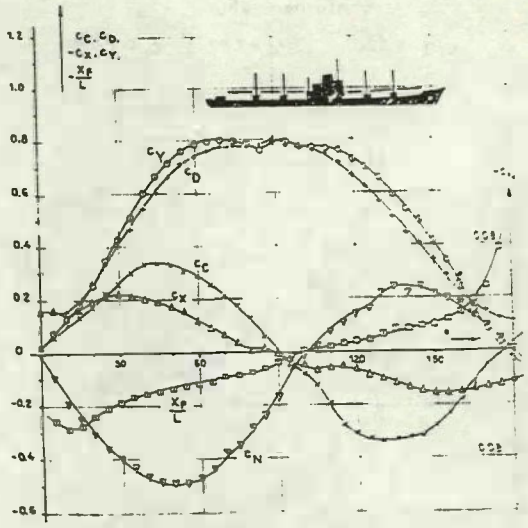

Fig.4.2 Example of Wind Tunnel Test Results /35/

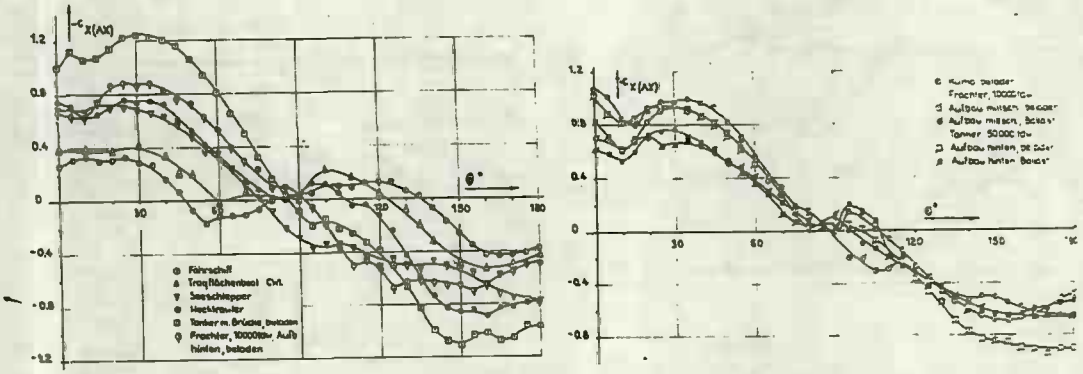

Fig.4.3 Example of Wind Resistance Coefficients as a Function of Incidence Angle /35/

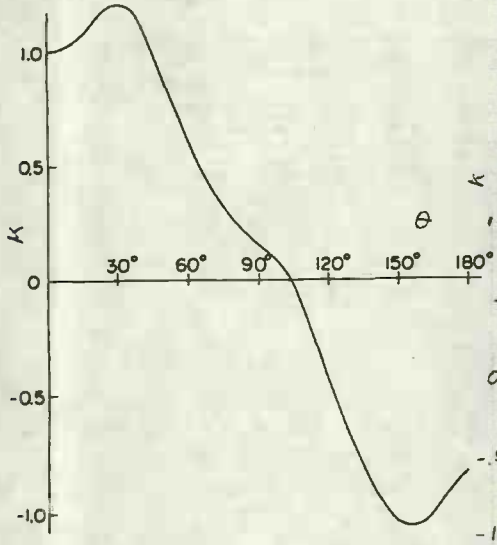


Fig.4.4 Head Resistance Coefficient Curve (1) /38/

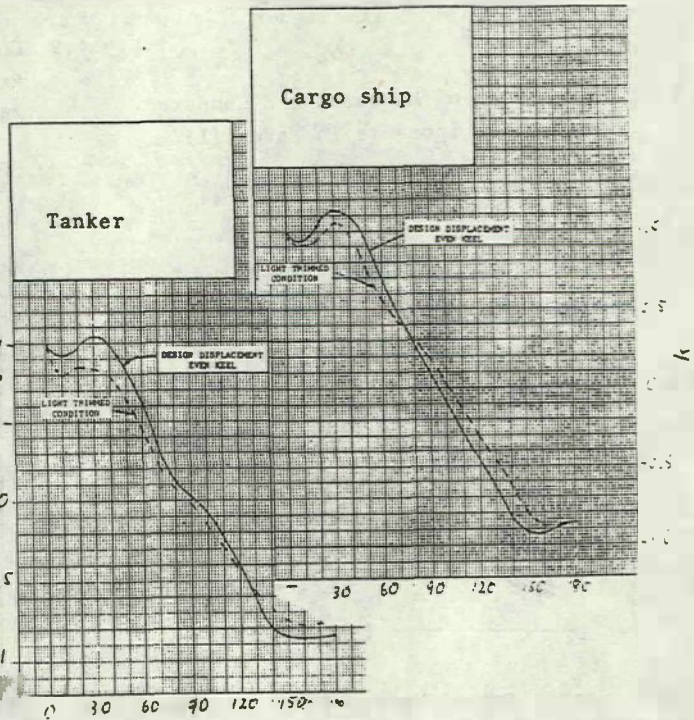


Fig.4.5 Head Resistance Coefficient Curve (2) /39/

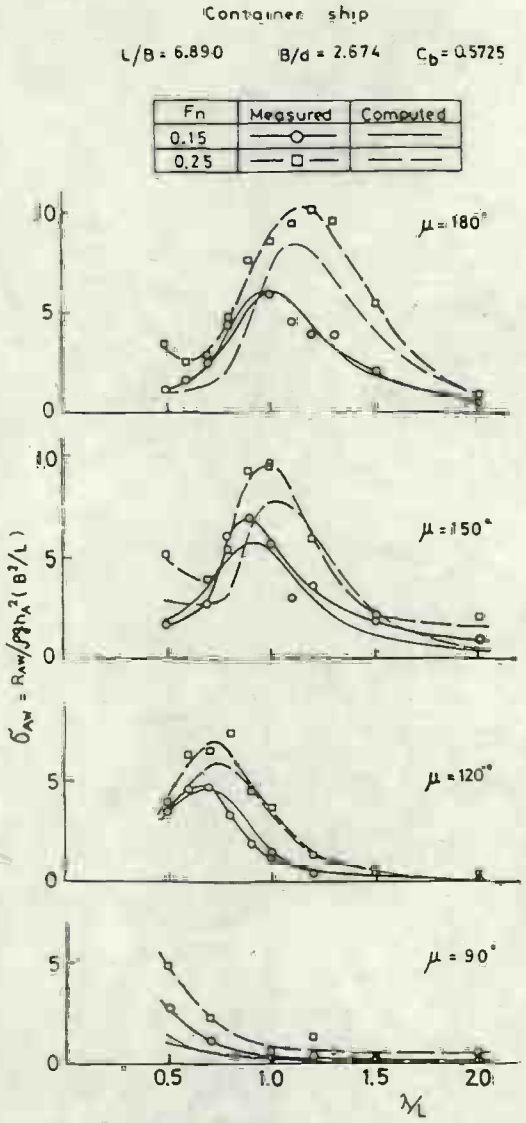


Fig.4.6 Comparison of Measured and Computed Resistance Increase in Waves (1) /45/

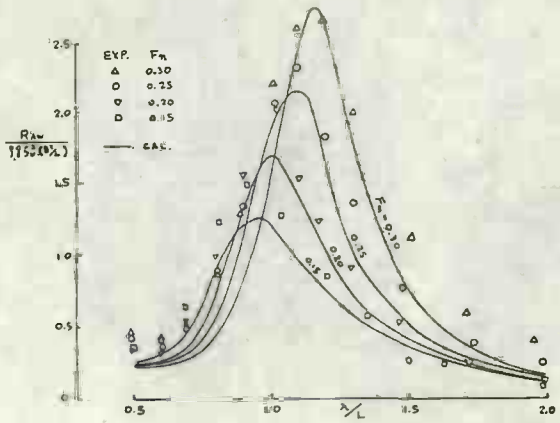


Fig.4.7 Comparison of Measured and Computed Resistance Increase in Waves (2) /46/

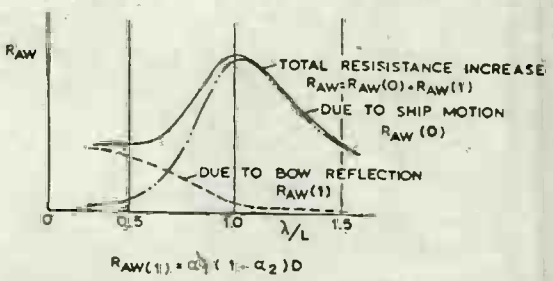


Fig.4.8 Components of Resistance Increase of Full Ships /45/

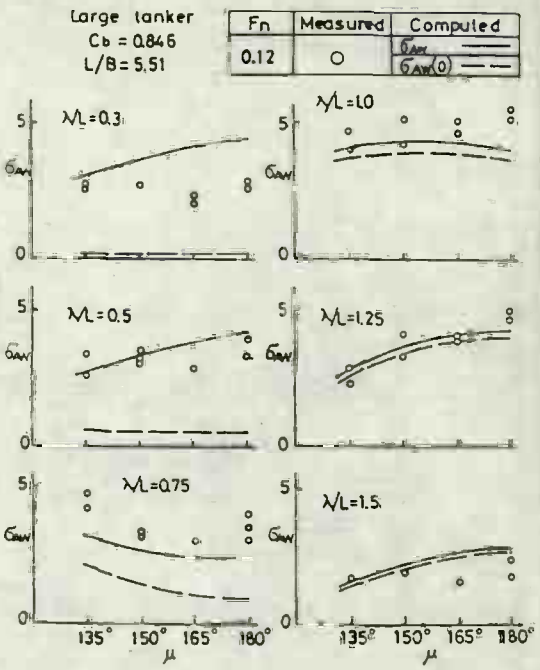


Fig.4.9 Comparison of Measured and Computed Resistance Increase in Waves (3) /47/

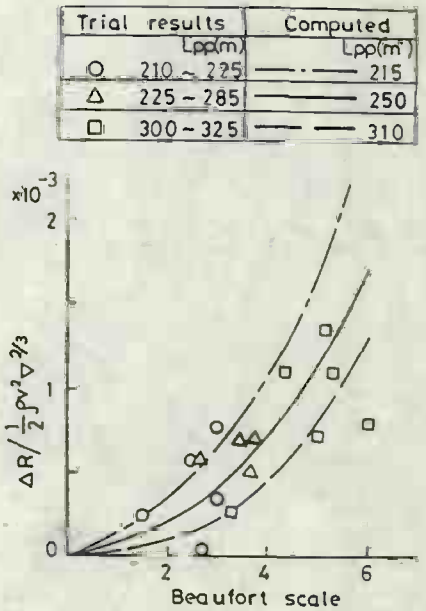


Fig.4.10 Resistance Increase in Waves Derived from Speed Trial Results/51/

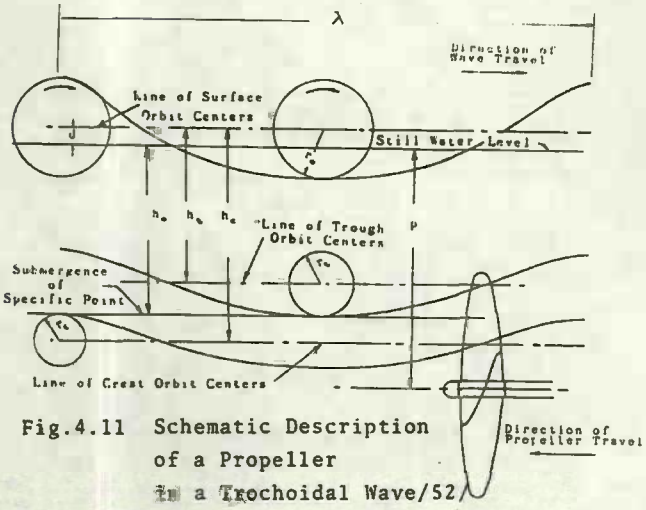


Fig.4.11 Schematic Description of a Propeller in a Trochoidal Wave/52/

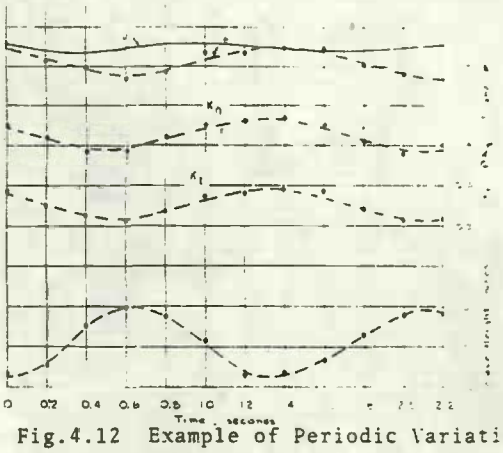


Fig.4.12 Example of Periodic Variation of Propeller Thrust and Torque in Waves /52/

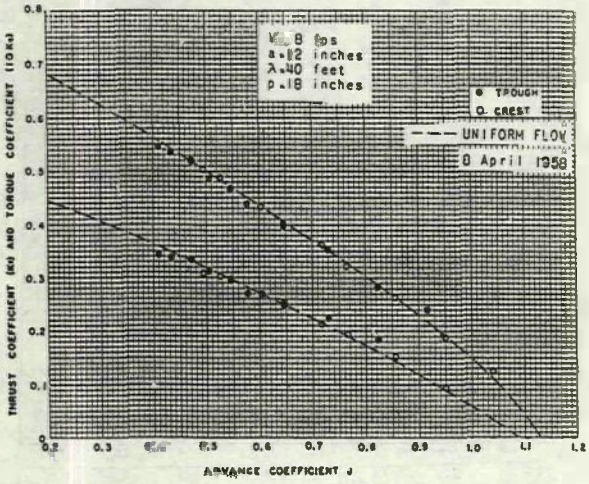


Fig.4.13 Max., Min. and Mean Thrust and Torque of a Propeller in Waves /52/

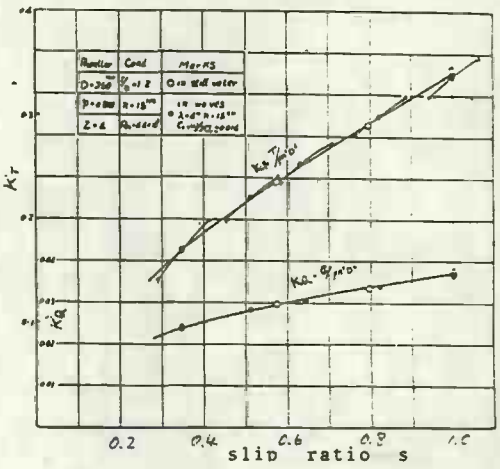


Fig.4.14 Max., Min. and Mean Thrust and Torque of a Propeller in Waves /53/

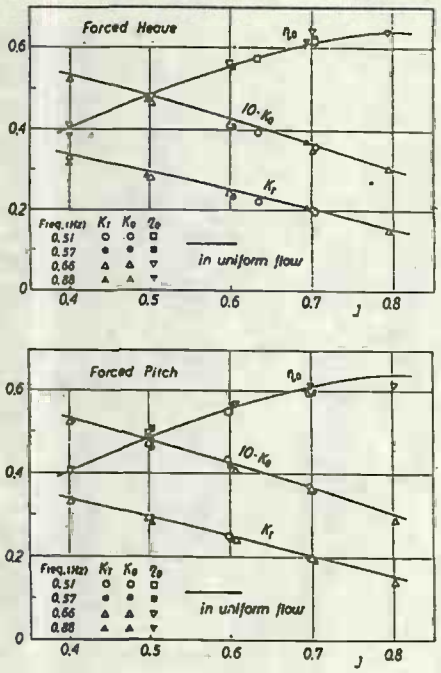


Fig.4.15 Open-Water Characteristics of a Propeller under Forced Motions /54/

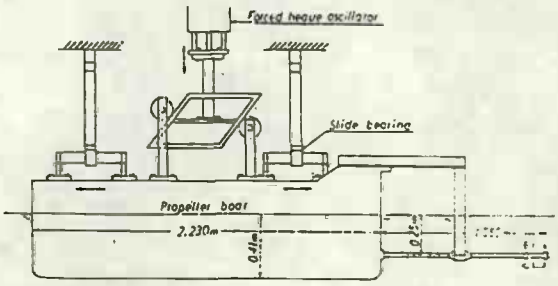


Fig.4.16 Test Set-up for Forced Motion of a Propeller in Open Water /54/

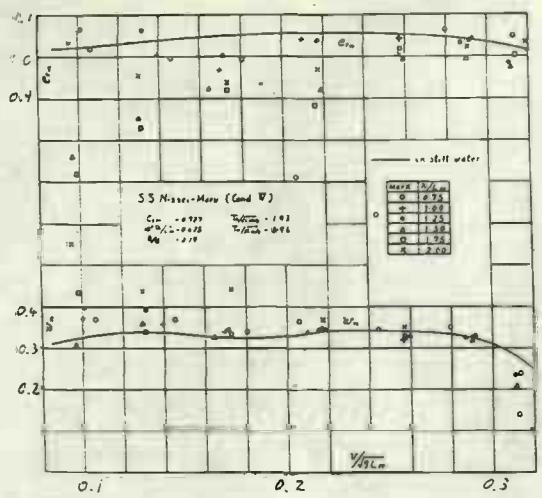

Fig.4.17 Self-Propulsion Factor in Waves
(1) Cargo Ship /53/

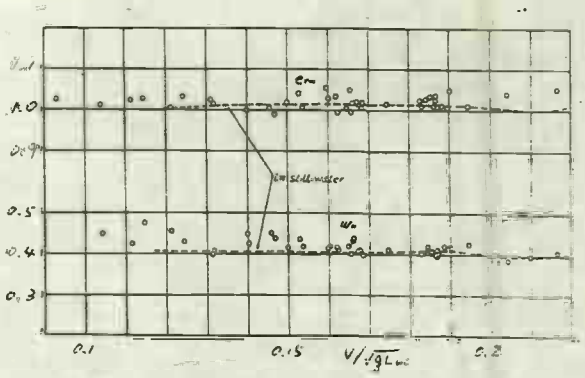

Fig.4.18 Self-Propulsion Factor in Waves
(2) Tanker /53/

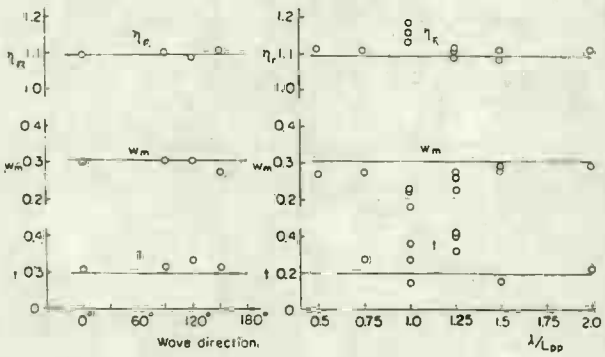

Fig.4.19 Self-Propulsion Factors in Waves
(3) Container Ship

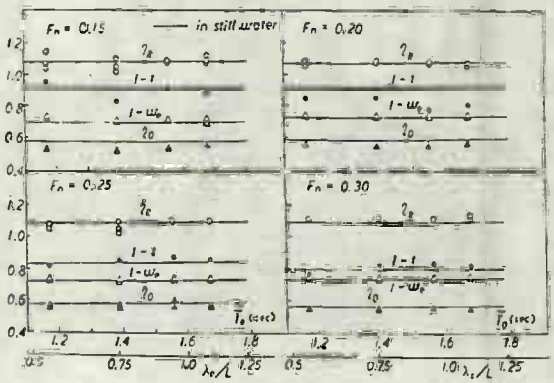

Fig.4.20 Self-Propulsion Factors in Waves
(4) Container Ship

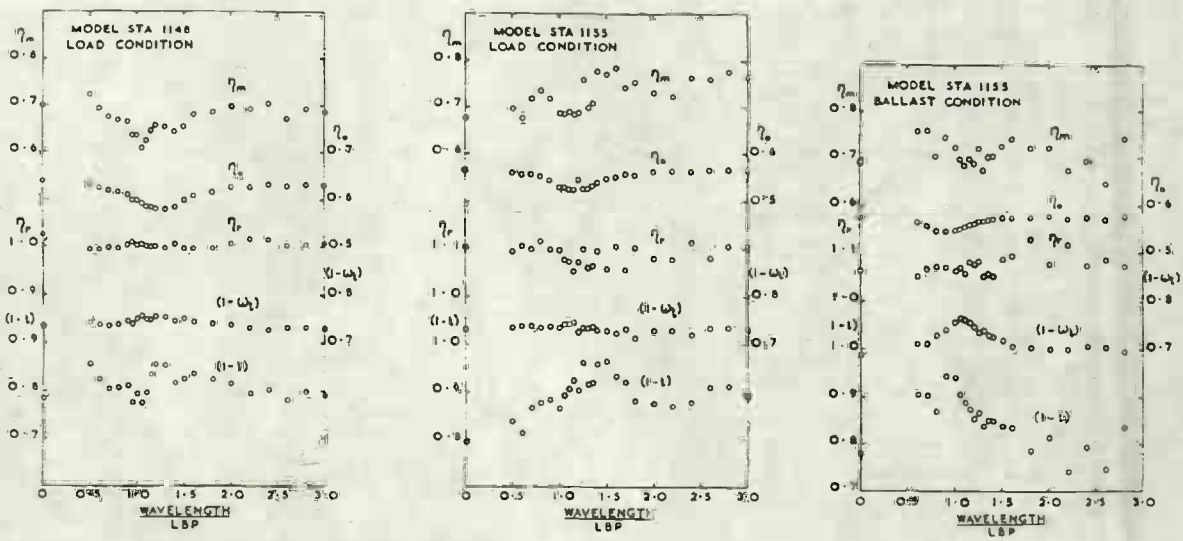

Fig.4.21 Self-Propulsion Factors in Waves (5) Cargo Ships /56/

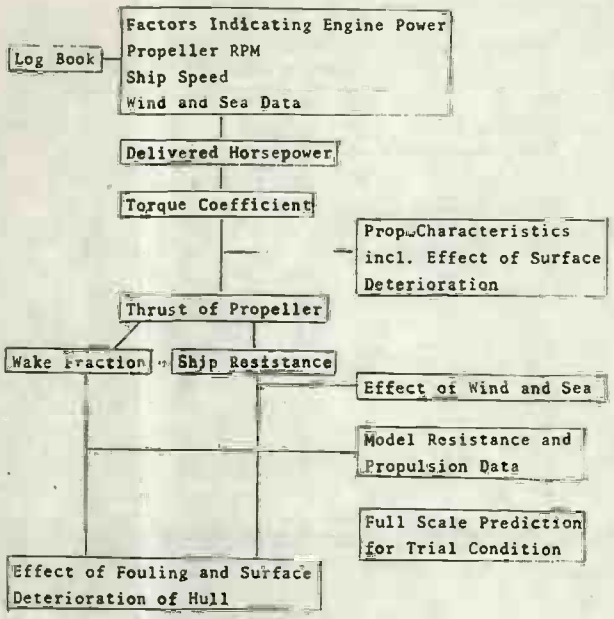


Fig.5.1 Analysis of Service Performance Data

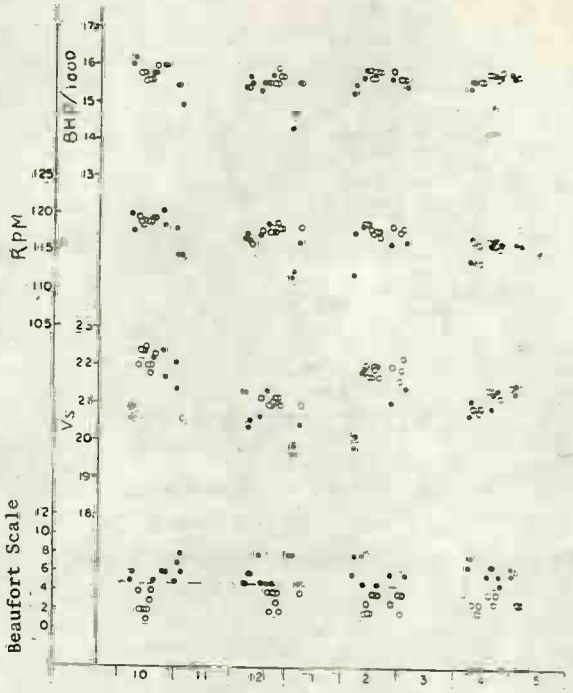


Fig.5.2 Example of Daily Data of Service Record

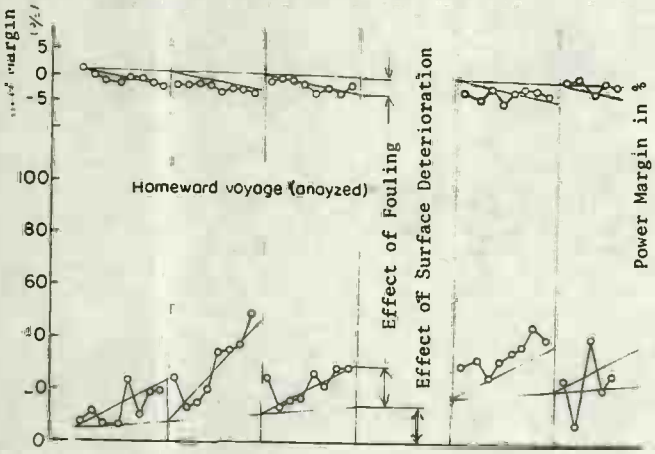


Fig. 5.3 Mean Values per Voyage for a Tanker /58/

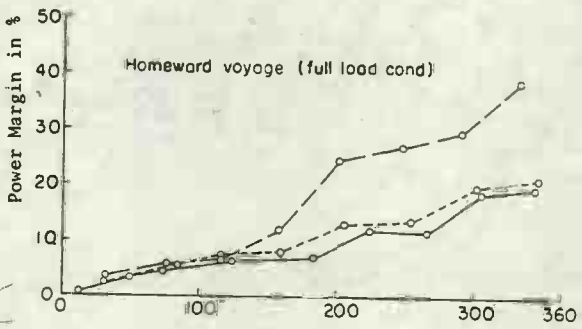


Fig.5.4 Fouling Effect Derived from Fig.5.3

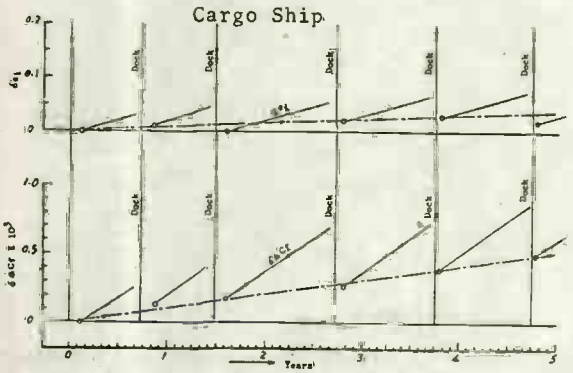


Fig.5.5 Effect of Fouling and Surface Deterioration Expressed by Change of $\Delta C_F$ and $W_S$ /59/

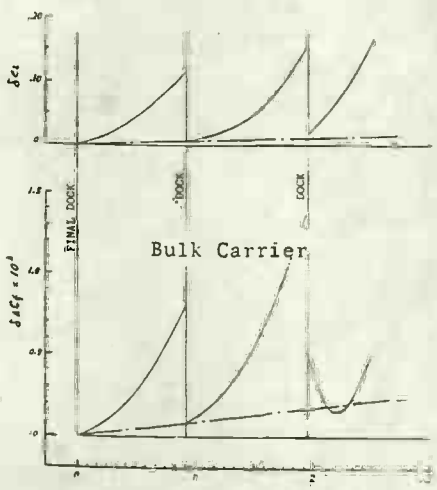


Fig.5.6 Similar to Fig.5.6 /59/

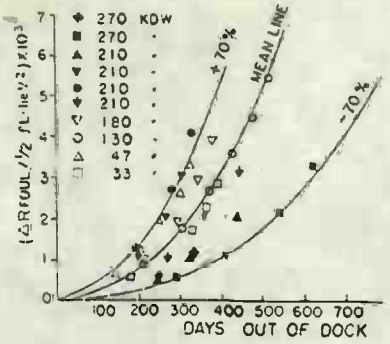


Fig.5.7 Effect of Fouling on Resistance Increase Derived from Service Record /60/

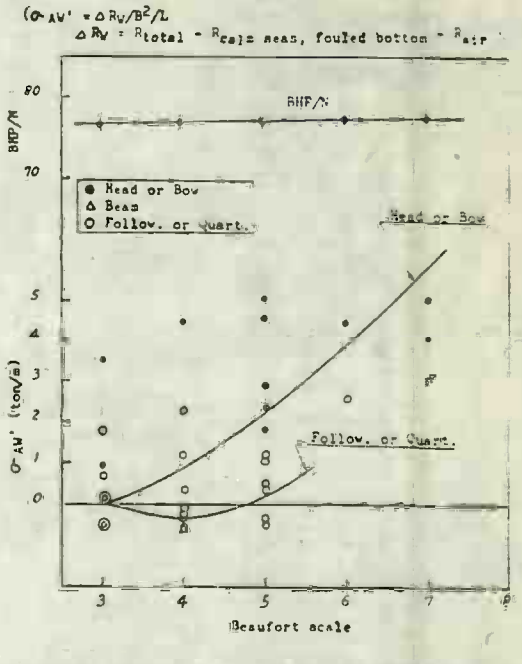


Fig.5.8 Resistance Increase in Waves Derived from Service Record /59/

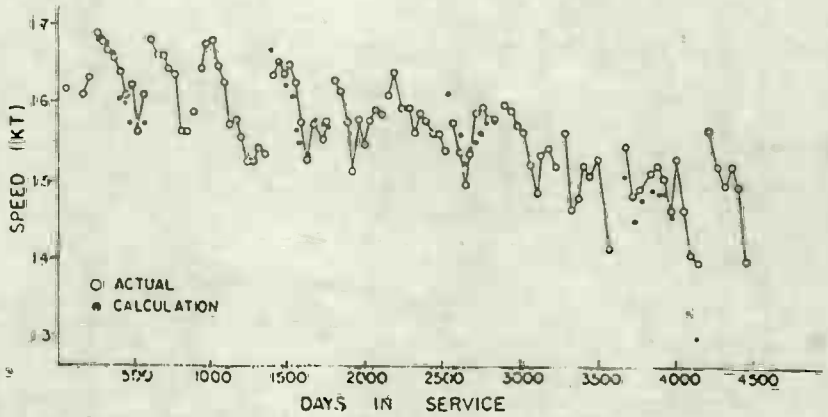


Fig.5.9 Example of Predicted Service Speed of a Ship Compared with Actual Performance Data /60/

TANIBAYASHI H., Dr. Eng.
Manager, Resistance & Propulsion Research Laboratory,
Nagasaki Experimental Tank
Mitsubishi Heavy Industries,Ltd.
3 - 48 Bunkyo-machi, Nagasaki 852, JAPAN